Dalton Transactions

Accepted Manuscript

This article can be cited before page numbers have been issued, to do this please use: W. Weigand, J. Hildebrandt, N. Haefner, H. Görls, D. Kritsch, G. Ferraro, M. Duerst, I. B. Runnebaum and A. Merlino, *Dalton Trans.*, 2016, DOI: 10.1039/C6DT01388K.

ROYAL SOCIETY OF CHEMISTRY

www.rsc.org/dalton

View Article Online
DOI: 10.1039/C6DT01388K

Platinum(II) O,S complexes as potential metallodrugs against Cisplatin resistance

Jana Hildebrandt,[a] Norman Häfner,[b] Helmar Görls,[a] Daniel Kritsch,[b] Giarita Ferraro,[c] Matthias Dürst,[b] Ingo B. Runnebaum,[b] * Antonello Merlino,[c,d] * and Wolfgang Weigand[a] *

* Prof. Dr. W. Weigand E-Mail: wolfgang.weigand@uni-jena.de

* Prof. Dr. A. Merlino E-Mail: antonello.merlino@unina.it

[a] Institut für Anorganische und Analytische Chemie Friedrich-Schiller-Universität Jena Humboldtstraße 8, 07743 Jena, Germany

[b]Department of Gynecology, Jena University Hospital - Friedrich Schiller University Jena

[c]Department of Chemical Sciences, University of Naples Federico II, Complesso Universitario di Monte Sant' Angelo, Via Cintia, I-80126, Napoli, Italy

[d]CNR Institute of Biostructures and Bioimages, Via Mezzocannone 16, I-80100, Napoli, Italy

AUTHOR EMAIL ADDRESSES (wolfgang.weigand@uni-jena.de antonello.merlino@unina.it)

RECEIVED DATE (to be automatically inserted after your manuscript is accepted if required according to the journal that you are submitting your paper to)

* To whom correspondence should be addressed. E-mail: wolfgang.weigand@uni-jena.de (W.W.), Fax: +49 3641 948102, Tel: +49 3641 948160, antonello.merlino@unina.it (A.M), Fax: +39 081674090, Tel: +39 081674276

View Article Online
DOI: 10.1039/C6DT01388K

Abstract We report on platinum(II) complexes with different cinnamic acid derivatives as ligands with cytotoxic activity against Cisplatin resistant ovarian cancer cell line subcultures of SKOV3 and A2780. Typical mechanism of actions for platinum(II) complexes as Cisplatin itself are binding to the DNA and inducing double-strand breaks. We examined the biological behavior of these potential drugs with 9-methylguanine using NMR spectroscopic methods and their DNA damage potential including γH2AX-foci analyses. X-ray diffraction methods have been used to elucidate the molecular structures of the platinum(II) complexes. Interactions with the model protein lysozyme have been evaluated by different techniques including Uv-Vis absorption spectroscopy, fluorescence and X-ray crystallography.

Keywords Cisplatin / 9-methylguanine /Cisplatin resistance / γH2AX-foci analyses / protein platination/ X-ray crystallography

Introduction

Cisplatin was first synthesized by Michele Peyrone in 1845 and its square planar configuration was demonstrated by Alfred Werner ca. 50 years later. [1-4] Its mechanism of action results in binding to the DNA, especially guanine, introducing strand crosslinks and causing DNA breaks during replication in proliferating cells (Figure 1). This results in an arrest of the cell cycle and to apoptosis of the affected cells as one of the main effects.[5-10] After intravenous application of the drug the delivery into the cells can be achieved by active transport via copper transporter or by passive diffusion.[11-13]

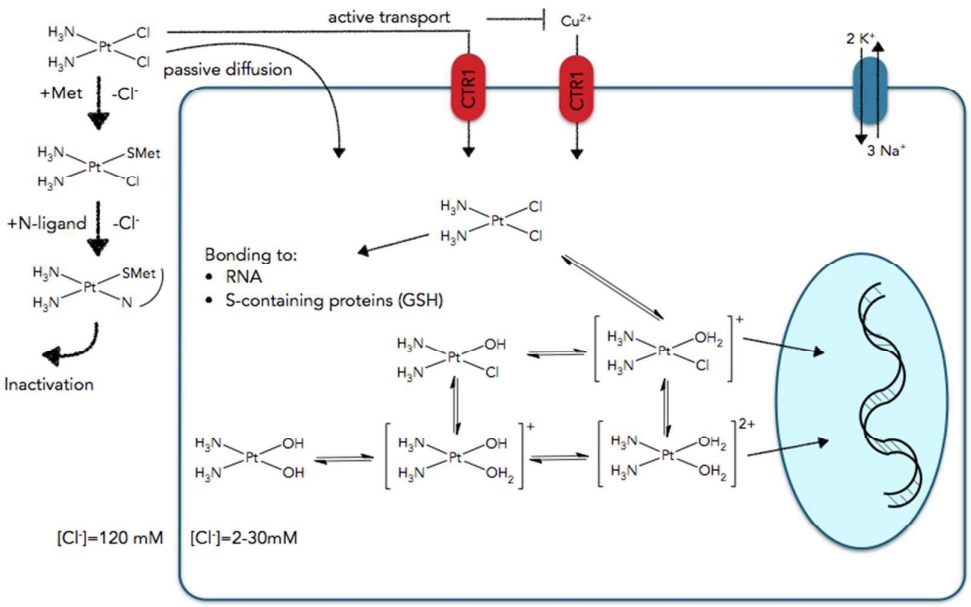

Figure 1. Behavior of Cisplatin after i.v. application: extracellular inactivation via binding to proteins (like albumin), active transport via copper transporter (CTR1) or passive diffusion into the cell and activation inside depending on lower Cl^- concentration $[Cl^-]$ to cationic aqua species which bind to genomic DNA.[4-12]

View Article Online
DOI: 10.1039/C6DT01388K

The lower intracellular chloride concentration compared to the blood plasma leads to ligand exchange reactions, in which the chlorido ligands of Cisplatin are substituted by aqua ligands.[14] This reaction generates the active platinum(II) species being able to bind to the DNA (Figure 1).[15, 16] Nevertheless, there are certain drawbacks in the anticancer therapy using Cisplatin: [17-27]

- low selectivity of this drug for tumor cells, resulting in severe side effects
- binding to extracellular albumin that leads to inactivation of the drug
- activity of DNA repair mechanisms may destroy the DNA Cisplatin adduct
- further principles of drug resistance of tumor cells.

The drug resistance, especially if caused by p-glycoprotein, is a major problem in treating diseases by pharmacological therapy.[28, 29] Moreover, it was shown that epigenetic changes in the cancer cells, if treated with sublethal concentrations of Cisplatin may contribute to the resistance phenotype.[30] All resistance mechanisms result in the lowering of Cisplatin effects and, in most cases, reduce the efficacy of a second treatment using Cisplatin. To solve these problems many substances of biological or synthetic origin were investigated concerning their use in cancer therapy. Targeted therapeutics offer an increased selectivity, but they are only suitable for specific cancer harboring the target. For other types of cancer, especially those that occur rarely, the use of Cisplatin is still the best way to treat them. It is noteworthy that even more selective drugs can lose their selectivity by changes of the genetic material of the tumor or of the tumor environment.[21, 26]

This work deals with the design of platinum(II) based drugs to circumvent Cisplatin resistance. One problem that has to be solved is the inactivation of Cisplatin by binding to sulfur-containing molecules like albumin in the blood plasma. It is known that platinum(II) exhibits a high affinity to sulfur atoms in organic molecules.[20, 31, 32] By binding to these sulfur sites, the drug molecules are excreted before they can bind to the DNA or even before they can pass the cell wall. For this reason there is a necessity to investigate the interactions of new platinum based drugs to proteins as well as the interactions with the DNA.[33]

View Article Online
DOI: 10.1039/C6DT01388K

Substance Code	Rest -R	Alkylgroup -Alk
L1/Pt1	-*o*-OCH_3	-methyl
L2/Pt2	-*m*-OCH_3	-methyl
L3/Pt3	-*p*-OCH_3	-methyl
L4/Pt4	-*o*-OCH_3	-ethyl
L5/Pt5	-*m*-OCH_3	-ethyl
L6/Pt6	-*p*-OCH_3	-ethyl
L7/Pt7	-*m*-OH	-methyl
L8/Pt8	-*p*-OH	-methyl
L9/Pt9	-*m*-OH	-ethyl
L10/Pt10	-*p*-OH	-ethyl
L11/Pt11	-H	-methyl
L12/Pt12	-H	-ethyl

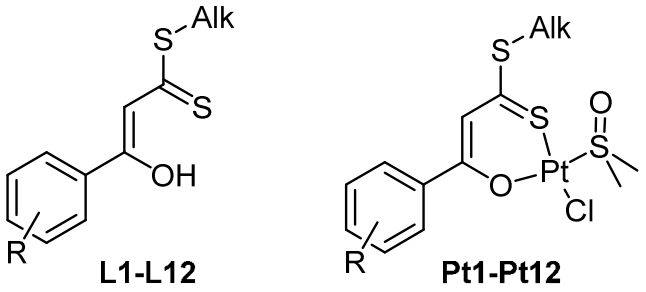

Figure 2. Scheme of synthesized ligands and platinum(II) complexes and its substance code with new platinum(II) complexes **Pt1**-**Pt6**.

Different types of β-hydroxy-dithiocinnamic acid derivatives were used as ligands. The properties of this class of compounds can be modified by changing the substitution pattern as well as the chain length of the alkyl substituent. As substituents for the aromatic moiety hydroxy and methoxy groups were used to vary the polarity of the ligand as well as of the platinum(II) complex. To investigate the effect of Cisplatin resistance, the cytotoxic activity of all compounds (β-hydroxy dithiocinnamic acid derivatives and the corresponding platinum(II) complexes) was tested with normal and Cisplatin resistant cell lines.

Figure 2 shows the used β-hydroxy dithiocinnamic acid derivatives and their corresponding platinum(II) complexes. Ligands **L1-L12** can be found in the literature, their cytotoxic effects were not determined until now.[33-39] Platinum(II) complexes **Pt7-Pt12** were reported earlier, this works presents first time biological significance of these compounds depending on their antitumor activity and reinvestigated what was reported earlier.[33, 40]

View Article Online
DOI: 10.1039/C6DT01388K

Results and Discussion

Synthesis

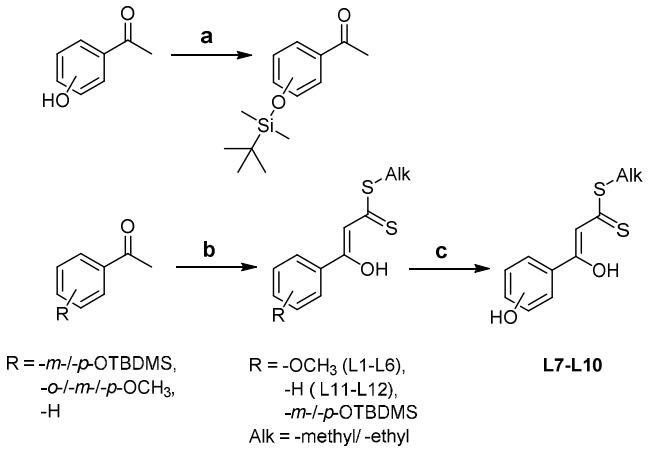

Scheme 1. Reagents and conditions: (a) (i) 2 equiv imidazole, 1 equiv TBDMS, DMF, rt, 24 h; (ii) H_2O/ $NaHCO_3$; (b) (i) 2 equiv *t*-BuOK, Et_2O, -70 °C, 0.5 h; (ii) 1.4 equiv CS_2, -70 °C, 1 h; (iii) rt, 1.5 h; (iv) 1 equiv Alk-I, rt, 24 h; (v) H_2SO_4/H_2O, rt, 0.5 h; (c) (i) 2 equiv TBAF, THF, rt, 72 h; (ii) H_2SO_4/H_2O, rt, 0.5 h.

Cinnamic acid derivatives **L1-L12** were synthesized according to modified literature methods.[34, 37-39] A general pathway is shown in Scheme 1.

For the synthesis of the platinum(II) complexes (Scheme 2) two pathways differing in the amount of *t*-BuOK can be applied. In absence of an aromatic -OH substituent one equivalent is used to deprotonate the cinnamic acid derivative. This intermediate is reacted with in situ generated $K[PtCl_3(dmso)]$ complex (prepared from K_2PtCl_4 and dmso).[33, 40-43] In presence of an aromatic -OH substituent the use of two equivalents of base results in higher yield of the desired platinum(II) complexes. This pathway needs an additional protonation step in the end.

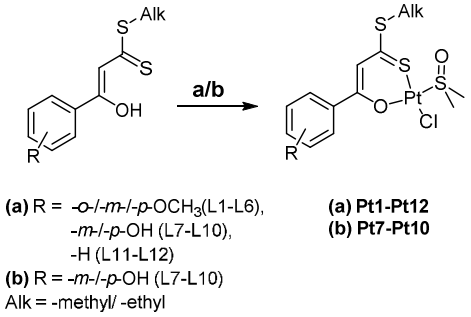

Scheme 2. Reagents and conditions: (a) (i) 1 equiv *t*-BuOK, THF, rt, 0.5 h; (ii) 1.1 equiv $K[PtCl_3(dmso)]$, rt, H_2O/THF, 96 h; (b) (i) 2 equiv *t*-BuOK, THF, rt, 0.5 h; (ii) 1.1 equiv $K[PtCl_3(dmso)]$, rt, H_2O/THF, 96 h; (iii) H_2SO_4/H_2O, rt, 0.5 h.

View Article Online
DOI: 10.1039/C6DT01388K

Molecular Structures

Platinum(II) complexes **Pt1-Pt3, Pt5-Pt7, Pt9** and **Pt10** as well as ligands **L1** and **L7** were characterized by means of single crystal X-ray structure determination, whereas the molecular structures of **Pt12, L3, L8** and **L11** are already known.[32, 36, 43] For compounds **Pt2, Pt3, Pt6, Pt9** and **L7** there are at least two independent molecules in their unit cells, but just one is shown. Bond lengths and angles are very similar for the molecules in a unit cell so that only one molecule is discussed below. All molecular structures are displayed in supporting information (Figure S1), Figure 3 shows as an example **Pt1** and **Pt7**.

In Figure 4 selected bond lengths and angles of the ligands **L1** and **L7** are presented. Both compounds offer a *cis* enol configuration due to intramolecular hydrogen bonding between the OH group and the adjacent thiocarbonyl moiety. Ligand **L1** displays a OH¬…S distance of 2.08 Å, which is quite similar to that of ligand **L7** with 2.05 Å. Results confirm data that were reported earlier.[36, 43] The C(1)-S(1) distance is a bit longer than that of a typical -C=S double bond (1.61 Å), C(2)-C(3) shows typical double bond character, whereas C(1)-C(2) distance is typical for a single bond. The bond lengths C(3)-O(1) are determined as 1.334(3) for **L1** and 1.3308(6) for **L7**. For the meta hydroxy substituted ligand **L7** the formation of intermolecular hydrogen bondings can be assumed (2.77 Å for molecule A, 2.74 Å for molecule B) (Figure 5). Furthermore in the molecular structure of **L1** an interaction of the methoxy substituent and the methine proton can be detected, which is expressed by a short distance (2.33 Å) of the oxygen atom of the methoxy-group and the methine proton.

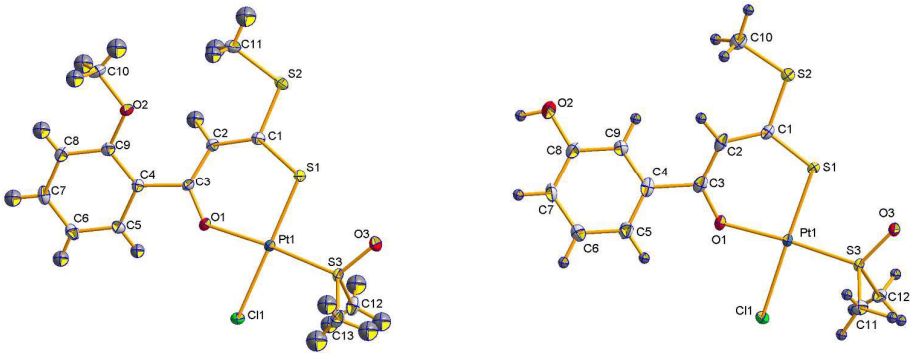

Figure 3. Molecule Structures (50% propability) of **Pt1** (left) and **Pt7** (right).

This proves an intramolecular interaction which results in a low field shift of the resonance signal of the methine proton in the ^{1}H NMR spectra in contrast to other β-hydroxy dithiocinnamic acid alkyl esters. Due to the steric demand of the meta-methoxy substituent in **L1** a torsion angle between the aryl ring and the planar enol moiety (C3/C2/C1/O1/S1/S2/C10) of 29° is detected, whereas in **L7** the same angle was determined as 4° (Figure 5).

View Article Online
DOI: 10.1039/C6DT01388K

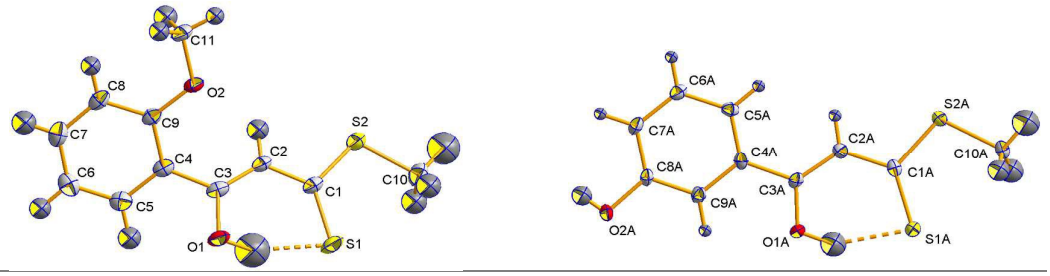

	L1	L7
C(1)-S(1)	1.681(2)	1.662(5)
C(3)-O(1)	1.334(3)	1.330(6)
C(1)-C(2)	1.424(3)	1.435(6)
C(2)-C(3)	1.368(3)	1.361(6)
C(9/8)-O(2)	1.364(3)	1.376(6)
O(1)-C(11)	1.439(3)	
C(3)-C(4)	1.476(3)	1.477(6)
C(1)-S(2)	1.739(3)	1.746(5)
C(2)-H(2)	0.94(3)	0.950(0)
S(1)-C(1)-C(2)	126.29(19)	125.2(4)
O(1)-C(3)-C(2)	123.2(2)	123.4(4)

Figure 4. Molecule Structures (50% propability) of **L1** (left) and **L7** (right) with specific bond angles [Å] and bond lengths [ppm].

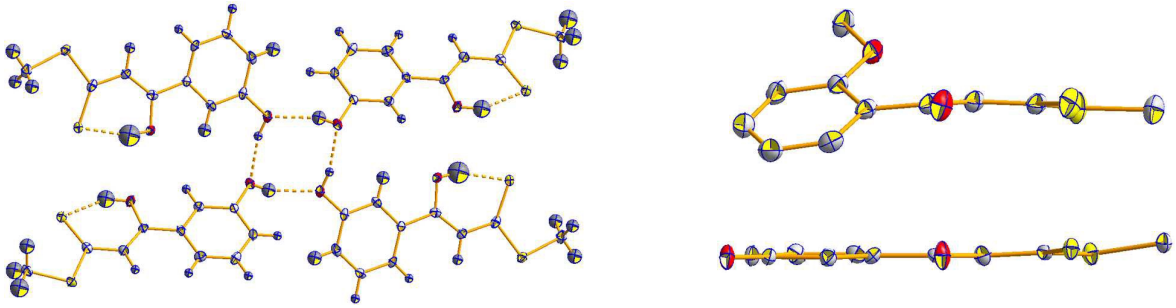

Figure 5. Left: Molecular packing of **L7**, intermolecular hydrogen-bonding; Right: Steric demand of methoxy-group resulting in non-planarity behaviour of **L1** (top) in comparison to the planar molecule **L7** (below).

The bond lengths and angles in the platinum(II) complexes **Pt1-Pt3**, **Pt5-Pt7**, **Pt 9** and **Pt10** are in good agreement with values reported earlier.[33] The platinum(II) center shows a distorted square planar environment with L-Pt-L angles of around 90° (see also Figure 3 and Table 1). The dmso coordination is *cis* to the sulfur atom of the bidendate O,S-ligand because of the π-donor-function of the sulfur atom. The bond lengths of platinum (here for example **Pt7**) and their four neighbor atoms are decreasing in the order of Cl(1)-Pt(1) (2.347(2)) > S(1)-Pt(1) (2.234(2)) ≈ S(3)-Pt(1) (2.189(2)) > O(1)-Pt(1) (2.014(6)). Moreover, the

View Article Online
DOI: 10.1039/C6DT01388K

angles of these coordination spheres are in the range of 90°. The bond lengths of the oxygen substituted moiety at the aromatic ring O(2)-C(9/8/7) are in the same range.

Table 1. Specific bond angles [Å] and bond lengths [ppm] for all characterized platinum(II) compounds.

	Pt1	**Pt2**	**Pt3**	**Pt5**
O(1)-Pt(1)	2.015(7)	1.985(10)	1.998(3)	2.007(4)
S(1)-Pt(1)	2.251(6)	2.251(3)	2.2556(13)	2.2520(14)
Cl(1)-Pt(1)	2.347(6)	2.338(3)	2.3595(13)	2.3463(13)
S(3)-Pt(1)	2.195(6)	2.198(3)	2.1846(12)	2.1934(14)
O(1)-C(3)	1.274(3)	1.282(18)	1.283(6)	1.287(7)
S(1)-C(1)	1.710(3)	1.690(14)	1.694(5)	1.701(6)
O(2)-C(9/8/7)	1.363(3)	1.298(17)	1.355(6)	1.368(7)
O(1)-Pt(1)-S(3)	175.10(5)	174.9(3)	174.44(11)	175.75(12)
S(3)-Pt(1)-Cl(1)	91.20(2)	90.05(12)	89.98(5)	89.84(5)
Cl(1)-Pt(1)-O(1)	84.13(5)	85.3(3)	84.48(11)	84.91(12)
S(1)-Pt(1)-S(3)	89.51(2)	89.10(13)	90.11(5)	89.84(5)

	Pt6	**Pt7**	**Pt9**	**Pt10**
O(1)-Pt(1)	2.003(5)	2.014(6)	2.017(3)	2.011(4)
S(1)-Pt(1)	2.2521(17)	2.234(2)	2.2439(10)	2.449(13)
Cl(1)-Pt(1)	2.3430(17)	2.347(2)	2.3520(10)	2.3359(13)
S(3)-Pt(1)	2.1865(17)	2.189(2)	2.1900(10)	2.1985(13)
O(1)-C(3)	1.280(8)	1.278(11)	1.284(5)	1.286(7)
S(1)-C(1)	1.700(7)	1.704(9)	1.700(4)	1.696(6)
O(2)-C(9/8/7)	1.361(8)	1.362(12)	1.351(6)	1.362(7)
O(1)-Pt(1)-S(3)	174.14(15)	174.97(19)	176.34(9)	175.11(11)
S(3)-Pt(1)-Cl(1)	90.08(6)	90.21(7)	90.96(4)	90.48(5)
Cl(1)-Pt(1)-O(1)	84.28(14)	85.96(17)	85.77(8)	84.99(11)
S(1)-Pt(1)-S(3)	89.63(6)	88.77(8)	87.96(4)	88.62(5)

Table 2 shows torsion angles (aryl planes and C(1)-C(2)-C(3) planes) which are resulting of the steric claim of different substitution pattern at the aromatic ring. The values show clearly that the smallest angle can be observed in case of the *para* substituted molecules.

Coordination of all O,S-chelating ligands to platinum(II) results in elongation of the C(1)-S(1) and shortening of the C(3)-O(1) bonds. This tendency can be also observed in $^{13}C\{^{1}H\}$-NMR spectra resulting in a high field shift of the signal of the -C=S-resonance and low field shift of the -C-O-group. For **Pt1** an interaction between the methoxy group and the methine proton is observed as for **L1**. The short O(2)-H(2) distance of 2.20 Å is indicative for the intramolecular relationship in these *ortho* substituted molecules.

The molecular structure of **L7** reveals that four molecules are connected through four hydrogen bonds forming an almost perfect square **Pt10** is able to form an intermolecular hydrogen bonding system (Figure 6). In the crystal there is a short contact between the hydroxy-group of one molecule and the oxygen of the dmso ligand of another molecule with a O-O distance of 2.73 Å.

View Article Online
DOI: 10.1039/C6DT01388K

Table 2. Torsion angles: angles between the aryl planes and C(1)-C(2)-C(3) planes in dependence of the substitution pattern.

	Pt1	Pt2	Pt3	Pt5	Pt6	Pt7	Pt9	Pt10
Torsion angle	30°	24°	17°	35°	7°	21°	31°	16°

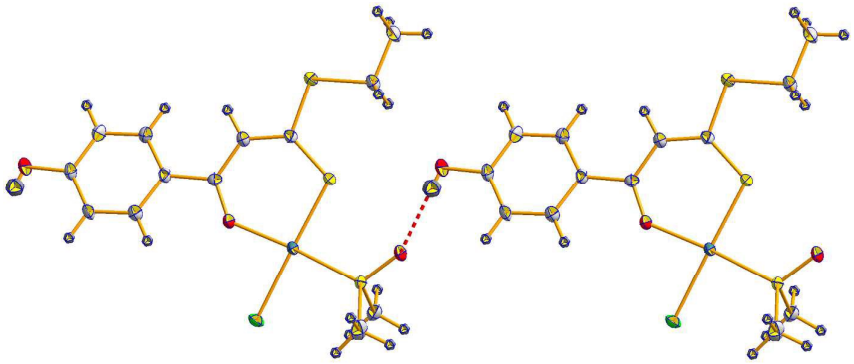

Figure 6. Intermolecular hydrogen-bonding observed in the crystals of **Pt10**.

Spectroscopic Characterization

All compounds were characterized by NMR spectroscopy, mass spectrometry and elemental analysis (see experimental part). The chemical shifts in ^{1}H NMR and ^{13}C{^{1}H} NMR spectra for ligands **L1-L12** are in good agreement with the values reported earlier, Table 3.[37] Interestingly the interaction of the *ortho* methoxy substituent and the methine proton that was found in the molecular structure of **L1** can be also detected in the ^{1}H NMR spectrum. The resonance signal of this proton is shifted to low field compared to those resonances of all other ligands, in which such interactions are not possible due to steric reasons. Another characteristic resonance signal in the ^{1}H NMR spectra of this type of compounds is caused by the enolic OH group and can be observed in some cases at very low frequencies at around 15 ppm. This also indicates the intramolecular hydrogen bondings to the sulfur atom of the thiocarbonyl moiety.

Table 3. Specific signals in NMR spectra of **L1-L12** and **Pt1-Pt12** in ppm.

^{1}H NMR	**L1 Pt1**	**L2 Pt2**	**L3 Pt3**	**L4 Pt4**	**L5 Pt5**	**L6 Pt6**	**L7 Pt7**	**L8 Pt8**	**L9 Pt9**	**L10 Pt10**	**L11 Pt11**	**L12 Pt12**
-C-O<u>H</u>	15.08		15.21	15.21	15.18	15.21	15.09		15.14	15.20	15.02	15.16
-C-<u>H</u>	7.20	6.97	6.98	7.23	6.91	6.91	6.96	6.88	6.91	6.91	6.89	6.90
	7.35	7.35	7.04	7.35	7.06	7.07	7.15	7.16	7.15	7.16	7.28	7.27
^{13}C{^{1}H} NMR	**L1 Pt1**	**L2 Pt2**	**L3 Pt3**	**L4 Pt4**	**L5 Pt5**	**L6 Pt6**	**L7 Pt7**	**L8 Pt8**	**L9 Pt9**	**L10 Pt10**	**L11 Pt11**	**L12 Pt12**
-<u>C</u>-OH	167.6	169.1	169.6	167.8	169.4	169.9	169.3	169.2	169.6	170.1	169.2	169.4
-C-<u>C</u>-H	112.9	112.9	107.1	112.8	112.9	106.8	113.8	106.8	113.8	106.9	107.8	107.7
	116.3	112.9	111.0	116.5	112.9	111.0	110.8	109.9	111.0	110.3	111.6	111.8
-<u>C</u>=S	217.2	217.3	215.7	216.3	217.3	214.9	217.8	215.8	217.1	215.2	217.3	216.3
	199.0	180.9	177.9	199.0	177.6	177.9	177.6	178.7	196.8	177.6	177.6	181.5

View Article Online
DOI: 10.1039/C6DT01388K

Specific shifts of $^{13}C\{^{1}H\}$ NMR and ^{1}H NMR resonance signals observable for the platinum(II) complexes are shown in Table 3. After complexation of the ligands via oxygen and sulfur atoms to platinum(II) the enolic OH signals in the ^{1}H NMR spectra disappear. Interestingly the signals of the methine protons are shifted to low frequencies as a result of their complexation to platinum(II). In the $^{13}C\{^{1}H\}$ NMR spectra the ^{13}C signal of the -C=S group can be observed at high frequencies for the platinum(II) compounds compared to those of the ligands. The protons of the dmso ligand are observed as a singlet accompanied with ^{195}Pt satellites in ^{1}H NMR spectra. The averages for these signals, which are presented with respect to the carbon side chains are shown in supporting information (Table S2).

Mass spectra are in common with earlier reported results.[33, 37, 40]

Stability Determination

Stability of compounds **Pt7** and **L8** in dmso as solvent were determined using ^{1}H NMR spectroscopy. For biological testing compounds were dissolved in dmso (see experimental part). Figure 7 shows exemplary aromatic signals for compound **Pt7** from start point (blue) and after 48 hours (red). It was observed that all compounds are stable under these conditions (for **L8**: Figure S2 in supporting information).

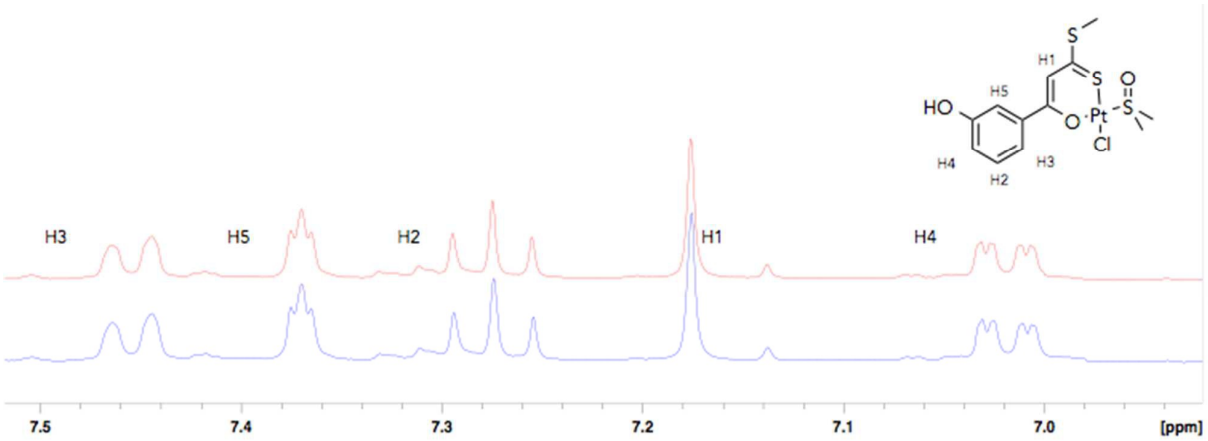

Figure 7. Stability determination of **Pt7** using ^{1}H NMR spectroscopy, Conditions: 600 MHz, 37 °C, dmso-d_6. Blue: first measurement (starting point), red: after 48 h. All compounds are stable under these conditions.

However, since it is well known that the behavior of metal based drugs in organic solvent like dmso could be different when compared to that observed in the solutions used for the biological studies, the stability of the platinum complexes here studied were assessed also in aqueous solutions (from 10 to 100 % dmso) using UV–Vis absorption spectroscopy.[44] In particular, the spectra of the compounds **Pt1**-**Pt6** were collected at t = 0 h and after 24 h. Analyses of the spectra show that the compounds **Pt1**-**Pt6** with the exception of Pt2, are highly stable in pure dmso (Figure S3A), and rather stable in 70-90% dmso. The reason why Pt2 is not so stable in pure dmso are unknown. On the contrary, they are less stable at low dmso concentrations (Figure S3C). For example **Pt1** is stable in 70-90% and pure dmso, in agreement with NMR data, whereas it presents a significant decrease in the intensity of the Uv-Vis absorption bands after 24 h in aqueous solutions with dmso ranging from 10 to 60%. This decrease is coincident with precipitation of the sample.

View Article Online
DOI: 10.1039/C6DT01388K

The stability of Pt complexes **Pt1-Pt6** was also assessed in a saline solution (0.9% NaCl, 1%<[dmso]<2%), and in the reference physiological buffer solution (10 mM PBS pH 7.4) (Figure S4). Under these experimental conditions, the complexes seem only marginally stable, since they rapidly precipitate, as occurs in aqueous solutions containing low dmso concentrations. These findings indicate that under these experimental conditions the integrity of the compounds could be compromised.

DNA-binding Behavior

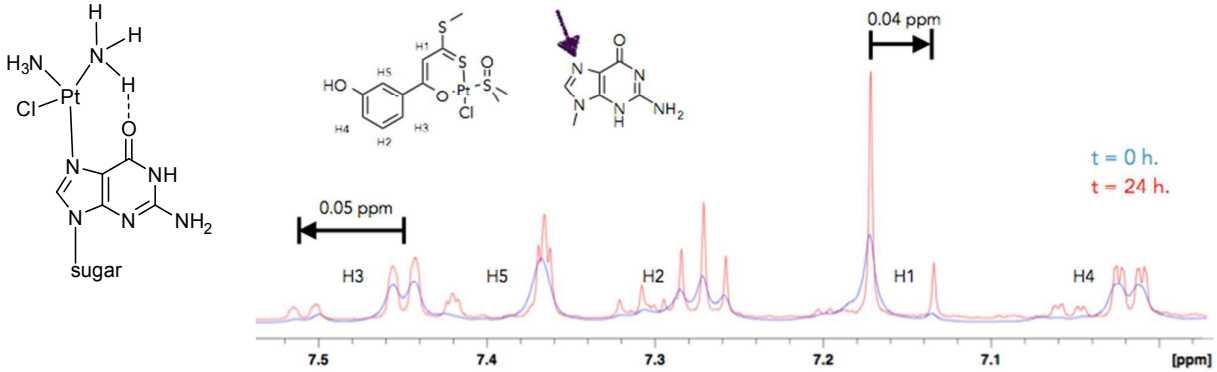

Figure 8. DNA-binding behaviour of Pt7 with model base 9-methylguanine shows formation of new compound after 24 h, 37 °C, 600 MHz, dmso-d_6; blue: start of measurement, red: after 24 h.

The cytotoxic behavior of Cisplatin and analogues is a result of binding to DNA bases i.e. guanine, influencing the DNA structure and causing DNA damage during genome replication. Preferred binding position is N7 of guanine because of a stabilization effect via hydrogen-bonding of Cisplatin -NH_3 group and -C=O-group of the DNA base (Figure 8).[5, 31] As shown in Figure 1, mechanism of activation contains a ligand-exchange of the chlorido ligands. Using ^{1}H NMR spectroscopy the binding properties of a 3.23-fold stoichiometric excess of the model base 9-methylguanine to platinum(II) compounds should be investigated. As shown in Figure 7, platinum(II) complexes are stable under these conditions, so all changes in the NMR spectra results from interaction with the model base. This NMR spectroscopic experiment carried out for compound **Pt7** monitored over 24 h at 37 °C in dmso-d_6 results in significant changes in this spectra. After 24 h the ^{1}H NMR spectra show in the aromatic region that a new compound is generated slowly, which can be seen by occurrence of a new set of proton signals for the methine proton as well as for all aromatic protons. The spectra show after 24 h a second proton group high field shifted (red spectrum, 0.05 ppm) compared to the signal set at t = 0 h (blue spectrum). In contrast, a down field shift (red spectrum) can be observed for the methine proton of **Pt7** after 24 h. These results give hint for a successful reaction of **Pt7** with 9-methylguanine however it seems that the reaction is slow and not completed after 24 h.

View Article Online
DOI: 10.1039/C6DT01388K

Biological Behavior

A further aim of our investigations was to characterize all of these compounds for their cytotoxic activity against a panel of cell lines enabling an interrogation of the structure – activity relationship. Used cell lines differed in their sensitivity against Cisplatin. Therefore candidate platinum(II) complexes potentially effective against Cisplatin resistant cells could be identified.

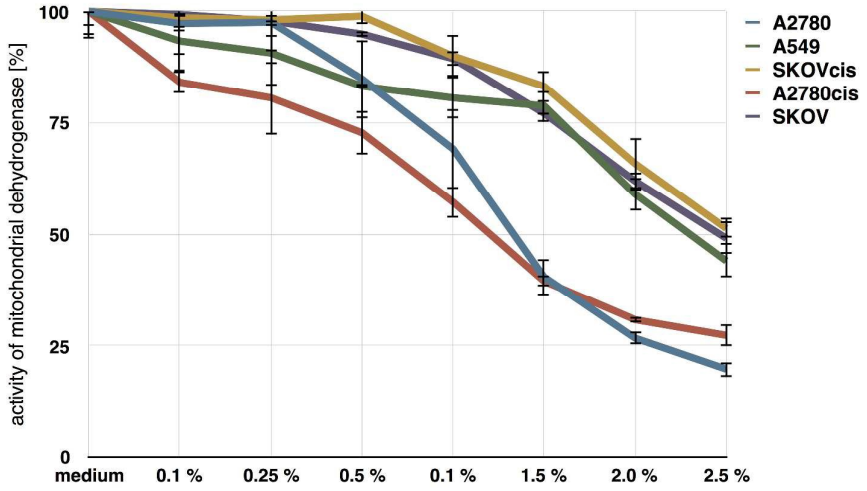

Figure 9. Influence of dmso depending on %/well for each cell line.

Analyzed ligands as well as platinum(II) complexes exhibit a low solubility in water independent from ligand structure. DMSO is used as a solvent for preparation of dilution series in cell culture experiments. The toxic influence of a range of dmso concentrations was measured via MTT assay under identical conditions as for substance tests (Figure 9). Results show that concentrations of dmso down to 1% have high cytotoxic effects. Therefore a dmso concentration as low as possible to reach required Pt(II) complex concentrations was used in the experiments and was identical for each substance and concentration (0.5% dmso in cell culture media). To exclude side effects from this dmso concentration all IC50 determination experiments used 0.5% dmso as reference samples. Additional experimental conditions can bias cell cultivation based IC50 determinations i.e. cell density, cultivation time and drug exposure time influence measured effects. High cell numbers (>5000 cells per well in 96-well plate) combined with long cultivation times (>72 h) may result in inhibitory effects on cell proliferation for samples with a low drug concentration and for control cells. Importantly any bias for cells even treated with drug concentrations different from IC50 will affect IC50 determination because regression analyses will interrogate all data. Thus we measured drug effects for 48 h exposure time after 24 h seeding of 5000 cells per well resulting in unsaturated cell density and absorbance measurements for untreated cells (data not shown). Both, constantly low dmso concentrations and controlled cultivation procedures represent important improvements in comparison to earlier data.[33, 40] Detailed experimental procedures are described in experimental part.

View Article Online
DOI: 10.1039/C6DT01388K

Table 4. IC50 values and resistance factors (RF) for all substances.

9	8	7	6	5	4	3	2	1	Substance code	Data
88.0 (+/- 5.6)	108.5 (+/- 11.8)	270.1 (+/- 18.0)	130.5 (+/- 12.9)	103.1 (+/- 10.5)	170.9 (+/- 20.0)	161.5 (+/- 24.2)	101.2 (+/- 9.2)	97.5 (+/-12.6)	**L**	**SKOV IC50**
23.5 (+/- 3.7)	50.5 (+/- 10.8)	26.3 (+/- 7.0)	12.2 (+/- 1.5)	14.3 (+/- 3.5)	75.7 (+/- 19.5)	35.5 (+/- 4.7)	28.8 (+/- 4.9)	35.0 (+/- 6.5)	**Pt**	
74.6 (+/- 5.9)	91.0 (+/- 0.7)	189.5 (+/- 15.0)	142.8 (+/- 23.8)	155.1 (+/- 41.6)	133.4 (+/- 26.2)	69.0 (+/- 2.2)	90.2 (+/- 3.1)	88.3 (+/- 18.3)	**L**	**SKOVcis IC50**
10.3 (+/- 5.9)	29.6 (+/- 7.7)	29.3 (+/- 7.8)	23.0 (+/- 5.8)	29.3 (+/- 2.2)	17.9 (+/- 3.7)	19.5 (+/- 0.6)	20.1 (+/- 3.0)	13.9 (+/- 4.4)	**Pt**	
0.8 0.4	0.8 0.6	0.8 1.1	1.1 1.9	1.5 2.0	0.8 0.2	0.5 0.4	0.9 0.7	0.9 0.4	**L** **Pt**	**RF SKOV**
54.3 (+/- 7.9)	60.4 (+/- 5.7)	63.2 (+/- 6.3)	64.6 (+/- 7.9)	37.1 (+/- 8.5)	56.3 (+/- 10.4)	53.3 (+/- 6.2)	53.0 (+/- 12.4)	64.8 (+/- 4.1)	**L**	**A2780 IC50**
10.3 (+/- 5.5)	29.1 (+/- 8.6)	17.7 (+/- 1.5)	23.1 (+/- 6.7)	25.6 (+/- 2.4)	33.9 (+/- 4.2)	18.7 (+/- 3.1)	19.8 (+/- 1.6)	13.2 (+/- 4.3)	**Pt**	
25.0 (+/- 4.6)	87.1 (+/- 3.0)	17.5 (+/- 2.0)	77.9 (+/- 6.2)	40.8 (+/- 8.5)	63.2 (+/- 11.3)	16.4 (+/- 3.7)	24.1 (+/- 7.2)	29.1 (+/- 6.8)	**L**	**A2780cis IC50**
10.1 (+/- 4.6)	23.5 (+/- 9.2)	17.4 (+/- 1.1)	9.3 (+/- 1.2)	20.2 (+/- 5.6)	39.1 (+/- 0.5)	20.1 (+/- 5.8)	21.0 (+/- 3.3)	13.4 (+/- 8.6)	**Pt**	
0.5 1.0	1.4 0.8	0.3 1.0	1.2 0.4	1.1 0.8	1.1 1.2	0.3 1.1	0.5 1.1	0.4 1.0	**L** **Pt**	**RF A2780**
144.5 (+/-31.4)	109.1 (+/- 20.1)	201.4 (+/- 29.3)	211.3 (+/- 63.5)	173.4 (+/- 8.6)	123.5 (+/- 1.9)	118.0 (+/- 26.8)	129.7 (+/- 13.6)	112.5 (+/- 34.8)	**L**	**A549 IC50**
14.6 (+/- 8.1)	32.0 (+/- 2.3)	20.0 (+/- 1.7)	38.1 (+/- 7.5)	9.1 (+/- 3.4)	93.0 (+/- 2.1)	32.7 (+/- 5.7)	24.2 (+/- 2.0)	34.4 (+/- 5.7)	**Pt**	

View Article Online
DOI: 10.1039/C6DT01388K

CDDP	12	11	10
3.8 (+/- 2.8)	43.9 (+/- 14.7)	112.0 (+/- 11.1)	95.4 (+/- 6.1)
	35.6 (+/- 1.5)	35.3 (+/- 6.4)	27.7 (+/- 6.4)
13.5 (+/- 4.4)	103.9 (+/- 17.8)	107.1 (+/- 7.5)	86.0 (+/- 11.4)
	20.4 (+/- 3.3)	22.7 (+/- 4.3)	15.2 (+/- 2.7)
3.6	2.4 0.6	1.0 0.6	0.9 0.5
1.3 (+/- 0.2)	37.1 (+/- 2.5)	38.8 (+/- 2.5)	39.1 (+/- 0.7)
	18.4 (+/- 4.1)	13.6 (+/- 3.5)	2.7 (+/- 0.6)
6.1 (+/- 2.1)	25.4 (+/- 7.6)	17.7 (+/- 1.0)	57.1 (+/- 4.5)
	23.0 (+/- 6.4)	13.5 (+/- 6.1)	3.5 (+/- 0.7)
4.7	0.7 1.3	0.5 1.0	1.5 1.3
7.6 (+/- 2.6)	86.6 (+/- 10.6)	57.9 (+/- 7.3)	94.6 (+/- 2.7)
	34.8 (+/- 4.0)	26.8 (+/- 0.5)	28.0 (+/- 5.5)

The tested cell line panel consisted of A549 (lung cancer) and two pairs of isogenic ovarian cancer cell lines with different Cisplatin sensitivity.[30]

Resistant ovarian cancer cells derived from A2780 and SKOV3 exhibited a 4.7 and 3.6 times higher IC50 value for Cisplatin, respectively. These cell cultures were established by repeated rounds of incubation with increasing Cisplatin concentrations starting with non-lethal concentrations.[30] Table 4 shows that the new substances show cytotoxic activity against all cell lines, not only for ovarian carcinoma cell lines SKOV and A2780. Determination for all pairs of ligand and platinum(II) complex prove that dithiocinnamic acid derivatives show low cytotoxic behavior itself and corresponding platinum(II) complex elevated cytotoxicity. It can be concluded, that the increased cytotoxic behavior of platinum(II) complexes is a result of the metal itself. An exception seems to be the cell line A2780cis exhibiting IC50 values similar between some ligands and their complexes (Table 4). Moreover a significant but weak correlation was identified between the IC50 of the ligand and the complex (Pearson correlation coefficient 0.301; $p<0.01$; Figure 10).

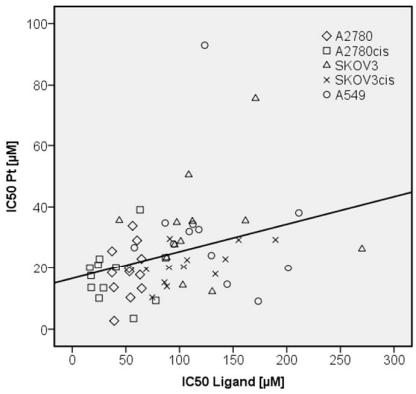

Figure 10. Correlation of ligand and platinum(II) complex IC50 values in all cell lines. The weak but significant correlation (Pearson r=0.301, p<0,001) is depicted by the regression line.

View Article Online
DOI: 10.1039/C6DT01388K

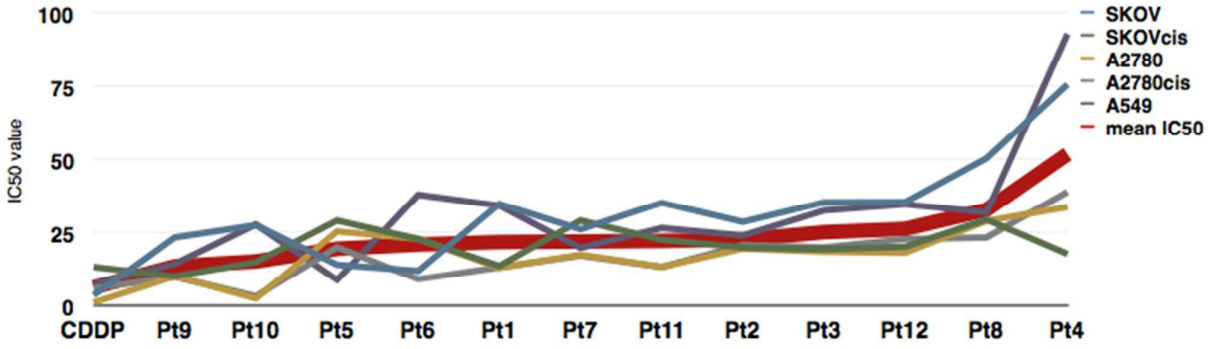

Figure 11. Structure activity relationship for analyzed platinum(II) complexes. Substances were ordered with increasing mean IC50 values.

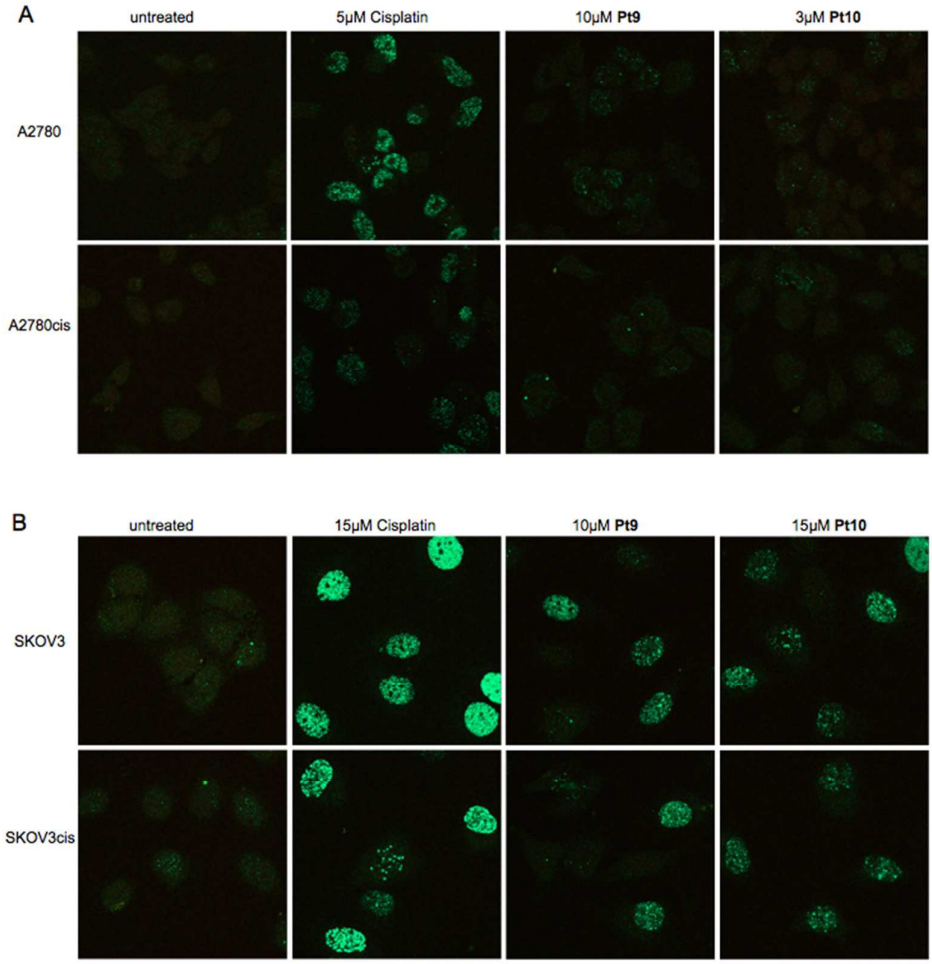

Figure 12. Detection of γH2AX foci in parental and Cisplatin resistant A2780 (A) and SKOV3 (B) after mock treatment or incubation with Cisplatin, **Pt9** or **Pt10** at IC50 concentrations for the resistant cells. Identical results were obtained in an independent experiment.

View Article Online
DOI: 10.1039/C6DT01388K

Thus a limited part of the platinum(II) complexes activity is maybe directly contributable to the ligand properties. One aim of the present study was to analyze structure-activity-relationships (SAR). Two structures within the analyzed ligands were systematically changed to vary complex properties (substituent at the benzyl ring (-R) and alkyl-chain at the sulfur residue (-Alk)). Plotting the IC50 values for all substances of each cell line in the order of increasing mean IC50 enabled the identification of SAR (Figure 11). Interestingly most active complexes exhibited an increased polarity of -R (-OH > -OCH_3 > -H) but increased lipophilicity at the alkyl chain (Et > Me). The exceptional cases of *ortho*-OCH_3 may be explained by intramolecular interactions between the methoxy group and the methine proton influencing the complex structures (see part molecular structures). Increased activity of complexes with longer alkyl chains confirms earlier studies.[33, 40] Nevertheless differences in the mean IC50 were small and substances exhibited cell line specific activities (i.e. **Pt9**, Figure 11). Interestingly, we did observe an inverse association between the platinum(II) complex stability and the cytotoxic activity. **Pt1** exhibiting a lower stability in aqueous solutions showed a higher cytotoxicity than **Pt4** (Figure 11, Table 4). Nevertheless the general impact should be determined in the *in-vivo* situation taking effects of the bioavailability into account.

The second aim was to test new platinum(II) complexes on Cisplatin-resistant cell lines to evaluate the possibility to overcome the resistance phenotype. The two most active platinum(II) complexes (**Pt9, Pt10**) showed an increased or at least equal cytotoxic activity against the Cisplatin-resistant ovarian cancer cell lines (Table 4). Moreover the activity was similar or even higher against the resistant cell lines in comparison to the parental cells. Calculated resistance factors between parental and resistant ovarian cancer cell lines (Table 4) illustrate clear differences between Cisplatin and some of the new platinum(II) complexes (i.e. RF Cisplatin 4.7 and 3.6; Pt9 1.0 and 0.4 for A2780 and SKOV3, respectively). These data let assume that the mechanism of action is different between the new compounds and Cisplatin. Moreover, a different kinetic cannot be excluded and is already seen within the guanine binding studies (see part DNA bonding behavior). Albeit we detected a high cytotoxic activity of the new complexes *in-vitro* an inactivation mechanism by binding to the tripeptide glutathion could not be excluded - for more information see supporting information (Figure S10). To gain insights into the mode of action we exemplarily analyzed **Pt9** and **Pt10** for the induction of DNA damage in the ovarian cancer cell line pairs in two independent experiments. Cells were incubated with IC50 concentrations of the resistant cell culture of A2780 or SKOV3 for 24 hours on cover slips. Afterwards cells were washed, fixed and antibody-stained for γH2AX histone. Nuclear foci of γH2AX are indicative for dsDNA break regions.[45] Cisplatin induced DNA damage and γH2AX foci formation clearly correlates with cytotoxic effects (Figure 12). Resistant cells showed decreased numbers of γH2AX foci. SKOV3 cells that are more resistant to Cisplatin than A2780 as illustrated by different IC50 values of 13.5 µM and 6.1 µM for the resistant cells, respectively, can tolerate increased γH2AX foci. The amount of γH2AX foci after treatment with **Pt9** or **Pt10** was much lower in comparison to the Cisplatin treatment despite all substances were used with IC50 concentrations (Figure 12). Therefore a different mode of action for the new platinum(II) complexes is likely and may include non-genomic targets. Otherwise it cannot be

View Article Online
DOI: 10.1039/C6DT01388K

excluded that the platinum(II) complexes show different kinetic behavior or target DNA differently from Cisplatin leading to other DNA damage responses not including γH2AX.

In conclusion platinum(II) complexes were proven to exhibit cytotoxic activities partially correlated to the ligand properties. The small differences in mean IC50 values enable a selection of the best candidates with both cytotoxic activity and superior bioavailability in future experiments (i.e. *in vivo*). Furthermore a high activity was detected for some substances against Cisplatin-resistant cell lines. Additional experiments will clarify the underlying mode of action for these platinum(II) complexes. If general differences to Cisplatin can be detected the efficacy of a combination treatment should be evaluated.

Interactions with proteins

Previous data show that the here investigated compounds show cytotoxic activity, especially **Pt9** and **Pt10** circumvent Cisplatin resistance (Table 4) but show decreased DNA damages (Figure 12). For this reason the discovery of other targets for their mechanism of action is necessary**.** The interaction of metallodrugs with proteins is very important, since it affects their pharmacokinetics, toxicity and tissue distribution. The binding of metal-based drugs with transferrin for example is directly involved in the transport of drugs into the cell. We have already demonstrated that compounds **Pt7** and **Pt9** are able to bind the model protein hen egg white lysozyme (HEWL) and the X-ray structure determinations of the adducts forming upon drug-protein interaction have been determined.[40] The structures demonstrate that the compounds can act as monofunction drugs, retaining dmso ligand upon macromolecule binding. To further characterize the binding properties of the compounds here studied with proteins, we have investigated the reactivity of compounds **Pt1-Pt6** with hen egg white lysozyme (HEWL), a protein that is very frequently used as a prototype for protein metalation studies.[46, 47]

First, fluorescence spectra of HEWL in the presence of different concentrations of the platinum complexes were collected. Intrinsic fluorescence of HEWL arise from the intrinsic structural features of the protein and is mainly due to the presence of six tryptophan residues. Figure S5 and Figure S6 show the modifications to the fluorescence emission of HEWL, upon excitation at 280 and 295 nm, respectively, when the **Pt1-Pt6** concentrations were increased. The binding of the drugs to the protein induces a significant quenching of the emission. Differences in the fluorescence quenching are probably related to different solubility of the samples rather than to differences in the binding properties of the compounds.

Finally, to identify the type of interaction that occur between HEWL and the Pt compounds we have tried to obtain structural information on the adducts formed by the protein with **Pt1-Pt4** by X-ray crystallography. Attempts to crystallize the adducts formed upon the binding of the compounds to the protein under the same conditions used to crystallize the HEWL-**Pt7** and HEWL-**Pt9** adducts failed.[40] This is probably due to the lower solubility of **Pt1**, **Pt2**, **Pt3**, and **Pt4** in ethylene glycol when compared to the compounds **Pt7** and **Pt9**, which present a-OH in meta position. Thus, the reactivity of the compounds with HEWL was explored under

View Article Online
DOI: 10.1039/C6DT01388K

different experimental conditions and the structures of some adducts formed in the presence of concentrated NaCl solutions were solved (see Supporting information Figure S7-S9). Under these experimental conditions Pt compounds degrade and the products of this degradation react with the protein forming an adduct with a Pt atom bound to ND1 atom of His15 side chain (see for example Figure S8), as in the case of many Pt compounds, including Cisplatin, **Pt7** and **Pt9** (see Supporting Information for further details).[40, 48-51]

Conclusion

The mechanism of action for standard drug Cisplatin is realized by DNA binding and induction of replicative stress resulting in DNA damage. This mechanism can be disturbed especially by the activity of DNA repair mechanism but also other mechanisms ending in the resistance of cancer cells. To circumvent Cisplatin resistance by the use of the effective Pt(II) pharmacophore was one aim of this work. Different ligands with varying properties and corresponding Pt(II) complexes were tested on several cell lines. Results show that the platinum(II) center is necessary for an effective anticancer activity. Examination of the mechanism of action shows that the typical DNA-binding behavior of Cisplatin and analogues and the induction of the DNA damage is decreased for the new Pt(II) complexes. Nevertheless some compounds have a high activity against Cisplatin resistant cell lines.

In summary, this work presents new platinum(II) complexes with O,S-bidendate ligands which are well characterized by different analytical techniques, especially with X-ray structure determinations. These complexes show cytotoxic activity partially overcoming Cisplatin resistance of cell lines which may be explained by a different mechanism of action - specifically the bonding to proteins.

View Article Online
DOI: 10.1039/C6DT01388K

Experimental Part

Materials and Techniques

All reactions were performed using standard Schlenk and vacuum-line techniques under nitrogen atmosphere. The NMR spectra were recorded with a Bruker Avance 200 MHz, 400 MHz or 600 MHz spectrometer. Chemical shifts are given in ppm with reference to $SiMe_4$. Mass spectra were recorded with a Finnigan MAT SSQ 710 instrument. Elemental analysis was performed with a Leco CHNS-932 apparatus. Silica gel 60 (0.015-0.040 mm) was used for column chromatography and TLC was performed using Merck TLC aluminium sheets (Silica gel 60 F_{254}). Chemicals were purchased from Fisher Scientific, Aldrich or Acros and were used without further purification. All solvents were dried and distilled prior to use according to standard methods.

Synthesis

General procedure 1: platinum(II)-complexes with β-hydroxy dithiocinnamic acid alkyl esters, chlorido and dmso as ligands (Pt1-Pt12).

Pathway A: The β-hydroxy dithiocinnamic acid alkyl ester (1 equiv) was solved in tetrahydrofurane (THF, 20 ml) and *t*-BuOK (1 equiv) was added to the the solution and stirred for one hour at room temperature. Potassium tetrachloroplatinate (K_2PtCl_4, 1.1 equiv) was solved in degassed water (10 ml) and dimethylsulfoxide (dmso, 2 equiv) was added, the mixture was stirred for 30 minutes at room temperature. The solution of the deprotonated ligand was added drop wise to the suspension of the platinum complex and stirred at room temperature for 4 days. After adding water (25 ml) to the solution, the mixture was extracted with dichlormethane (DCM, 3x 30 ml), the combined organic phases were washed with water (3x20 ml), dried over sodium sulfate and after filtration and evaporation of the solvent the crude product was purified with column chromatography. Pathway B: Experimental procedure is similar to pathway A, for deprotonation 2 equiv of *t*-BuOK was used. Before extracting with DCM, sulfuric acid (20 ml, 2M) was added and mixture was stirred one hour at room temperature followed by extraction and purification.

Chloro-(1-(2-methoxyphenyl)-3-(methylthio)-3-thioxo-prop-1-en-1-olate-*O,S*)-(dimethylsulfoxide-*S*)-platinum(II) (Pt1).

Synthesis was performed according to general procedure 1, pathway A. L1 (367 mg, 1.53 mmol) was dissolved in THF, *t*-BuOK (172 mg, 1.53 mmol) was added. K_2PtCl_4 (700 mg, 1.69 mmol) was dissolved in water, dmso (220 µL, 3.07 mmol) was added. Column chromatographie mobile phase: DCM 4:hexane 1 - DCM - acetone. Yield: 520 mg (62.1%) as red crystals. ^{1}H NMR (600 MHz, acetone-d_6): δ = 2.65 (s, 3H, -S-CH_3); 3.66 (s w/Pt satellites $^3J_{Pt\text{-}H}$=22.5 Hz, 6H, CH_3 (DMSO)); 3.94 (s, 3H, -OCH_3); 7.04 (ddd, $^3J_{H\text{-}H}$=7.6 Hz, $^4J_{H\text{-}H}$=1.0 Hz, 1H, -Ar-*m*-H); 7.13 (d, $^3J_{H\text{-}H}$=8.4 Hz, 1H, -Ar-*o*-H); 7.35 (s, 1H, =CH); 7.53 (ddd, $^3J_{H\text{-}H}$=7.6 Hz, $^4J_{H\text{-}H}$=1.0 Hz, 1H, -Ar-*p*-H); 7.80 (dd, $^3J_{H\text{-}H}$=7.8 Hz, $^4J_{H\text{-}H}$=1.8 Hz, 1H, Ar-*m*-H). ^{13}C{^{1}H} NMR

View Article Online
DOI: 10.1039/C6DT01388K

(101 MHz, acetone-d_6): δ = 17.7 (-S-CH_3); 46.7 (DMSO); 56.4 (-OCH_3); 113.3 (-Ar-*o*-C); 116.3 (=CH); 121.7 (-Ar-*m*-C); 128.0 (-Ar-C1); 132.1 (-Ar-*m*-C); 133.8 (-Ar-*p*-C); 158.3 (-Ar-OCH_3); 175.0 (-C-O-); 199.0 (-C=S). MS (DEI): m/z = 548, 546, 386, 341, 284, 152, 135, 105, 78, 63. Elemental analysis: calculated for $C_{13}H_{17}ClO_3PtS_3$·2/3 acetone C: 30.71%; H: 3.60%; S: 16.40%, found: C: 30.82%; H: 3.32%; S: 16.71%.

Chloro-(1-(3-methoxyphenyl)-3-(methylthio)-3-thioxo-prop-1-en-1-olate-*O,S*)-(dimethylsulfoxide-*S*)-platinum(II) (Pt2).

Synthesis was performed according to general procedure 1, pathway A. L2 (367 mg, 1.53 mmol) was dissolved in THF, *t*-BuOK (172 mg, 1.53 mmol) was added. K_2PtCl_4 (700 mg, 1.69 mmol) was dissolved in water, dmso (220 µL, 3.07 mmol) was added. Column chromatographie mobile phase: DCM 4:hexane 1 - DCM - acetone. Yield: 350 mg (41.8%) as orange crystals. ^{1}H NMR (400 MHz, $CDCl_3$): δ = 2.70 (s, 3H, -S-CH_3); 3.68 (s w/Pt satellites $^3J_{Pt\text{-}H}$=22.5 Hz, 6H, CH_3 (DMSO)); 3.88 (s, 3H, -OCH_3); 7.10 (dd, $^3J_{H\text{-}H}$=8.2 Hz, $^4J_{H\text{-}H}$=0.8 Hz, 1H, -Ar-*p*-H); 7.28 (s, 1H, =CH); 7.32 (t, 1H, -Ar-*m*-H); 7.54 (m, 2H, -Ar-*o*-H). ^{13}C{^{1}H} NMR (101 MHz, $CDCl_3$): δ = 17.6 (-S-CH_3); 46.9 (DMSO); 55.5 (-OCH_3); 112.9 (=CH); 118.3 (-Ar-*o*-C); 129.7 (-Ar-*m*-C/-Ar-C1); 135.7 (-Ar-*p*-H); 159.9 (-Ar-OCH_3); 174.2 (-C-O-); 180.9 (-C=S). MS (ESI): m/z = 565, 536, 512, 445, 101. Elemental analysis: calculated for $C_{13}H_{17}ClO_3PtS_3$·1/5 acetone C: 29.19%; H: 3.27%; S: 17.19%, found: C: 29.46%; H: 2.90%; S: 17.10%.

Chloro-(1-(4-methoxyphenyl)-3-(methylthio)-3-thioxo-prop-1-en-1-olate-*O,S*)-(dimethylsulfoxide-*S*)-platinum(II) (Pt3).

Synthesis was performed according to general procedure 1, pathway A. L3 (367 mg, 1.53 mmol) was dissolved in THF, *t*-BuOK (172 mg, 1.53 mmol) was added. K_2PtCl_4 (700 mg, 1.69 mmol) was dissolved in water, dmso (220 µL, 3.07 mmol) was added. Column chromatographie mobile phase: DCM 4:hexane 1 - DCM - acetone. Yield: 350 mg (41.8%) as orange crystals.. ^{1}H NMR (600 MHz, $CDCl_3$): δ = 2.60 (s, 3H, -S-CH_3); 3.59 (s w/Pt satellites $^3J_{Pt\text{-}H}$=22.5 Hz, 6H, CH_3 (DMSO)); 3.78 (s, 3H, -OCH_3); 6.84 (d, $^3J_{H\text{-}H}$=9.0 Hz, 2H, -Ar-*o*-H); 7.04 (s, 1H, =CH); 7.91 (d, $^3J_{H\text{-}H}$=9.0 Hz, 2H, -Ar-*m*-H). ^{13}C{^{1}H} NMR (101 MHz, $CDCl_3$): δ = 22.3 (-S-CH_3); 46.8 (DMSO); 55.5 (-OCH_3); 111.0 (=CH); 114.1 (-Ar-*o*-C); 129.4 (-Ar-*m*-C); 130.3 (-Ar-*m*-C); 163.0 (-Ar-OCH_3); 174.2 (-C-O-); 177.9 (-C=S). MS (ESI): m/z = 565, 536, 512, 445, 101. Elemental analysis: calculated for $C_{13}H_{17}ClO_3PtS_3$·1/2 acetone C: 30.18%; H: 3.49%; S: 16.67%, found: C: 30.57%; H: 3.18%; S: 16.18%.

Chloro-(1-(2-methoxyphenyl)-3-(ethylthio)-3-thioxo-prop-1-en-1-olate-*O,S*)-(dimethylsulfoxide-*S*)-platinum(II) (Pt4).

Synthesis was performed according to general procedure 1, pathway A. L4 (389 mg, 1.53 mmol) was dissolved in THF, *t*-BuOK (172 mg, 1.53 mmol) was added. K_2PtCl_4 (700 mg, 1.69 mmol) was dissolved in water, dmso (220 µL, 3.07 mmol) was added. Column chromatographie mobile phase: DCM 4:pentane 1 -

View Article Online
DOI: 10.1039/C6DT01388K

DCM - DCM 2:acetone1- -acetone. Yield: 516 mg (60.0%) as red oil. ^{1}H NMR (600 MHz, acetone-d_6): δ = 1.43 (t, 3H, -S-CH_2-CH_3); 3.23 (q, 2H, -S-CH_2-); 3.65 (s w/Pt satellites $^{3}J_{Pt-H}$=22.5 Hz, 6H, CH_3 (DMSO)); 3.94 (s, 3H, -OCH_3); 6.99 (ddd, $^{3}J_{H-H}$=7.6 Hz, $^{4}J_{H-H}$=1.0 Hz, 1H, -Ar-*m*-H); 7.14 (d, $^{3}J_{H-H}$=8.4 Hz, 1H, -Ar-*o*-H); 7.35 (s, 1H, =CH); 7.50 (ddd, $^{3}J_{H-H}$=7.6 Hz, $^{4}J_{H-H}$=1.0 Hz, 1H, -Ar-*p*-H); 7.62 (dd, $^{3}J_{H-H}$=7.8 Hz, $^{4}J_{H-H}$=1.8 Hz, 1H, Ar-*m*-H).^{13}C{^{1}H} NMR (101 MHz, acetone-d_6): δ = 13.7 (-S-CH_2-CH_3); 26.1 (-S-CH_2-); 46.7 (DMSO); 56.4 (-OCH_3); 112.9 (-Ar-*o*-C); 116.5 (=CH); 121.7 (-Ar-*m*-C); 129.3 (-Ar-C1); 130.6 (-Ar-*m*-C); 133.8 (-Ar-*p*-C); 158.3 (-Ar-OCH_3); 175.3 (-C-O-); 199.0 (-C=S).MS (ESI): m/z = 525, 448, 393, 337, 331, 245, 205, 173, 151.

Elemental analysis: calculated for $C_{14}H_{19}ClO_3PtS_3$·2/3 pentane C: 33.62%; H: 5.86%; S: 15.54%, found: C: 33.23%; H: 5.39%; S: 15.25%.

Chloro-(1-(3-methoxyphenyl)-3-(ethylthio)-3-thioxo-prop-1-en-1-olate-*O,S*)-(dimethylsulfoxide-*S*)-platinum(II) (Pt5).

Synthesis was performed according to general procedure 1, pathway A. L5 (389 mg, 1.53 mmol) was dissolved in THF, *t*-BuOK (172 mg, 1.53 mmol) was added. K_2PtCl_4 (700 mg, 1.69 mmol) was dissolved in water, dmso (220 µL, 3.07 mmol) was added. Column chromatography mobile phase: DCM 4:hexane 1 - DCM - DCM 2:acetone1- -acetone. Yield: 160 mg (18.6%) as yellow crystals. ^{1}H NMR (400 MHz, $CDCl_3$): δ = 1.43 (t, 3H, -S-CH_2-CH_3); 3.26 (q, 2H, -S-CH_2-); 3.64 (s w/Pt satellites $^{3}J_{Pt-H}$=22.5 Hz, 6H, CH_3 (dmso)); 3.84 (s, 3H, -OCH_3); 7.06 (m, 2H, -Ar-*p*-H/=CH); 7.29 (t, 1H, -Ar-*m*-H); 7.50 (m, 2H, -Ar-*o*-H).^{13}C{^{1}H} NMR (400 MHz, $CDCl_3$): δ = 14.0 (-S-CH_2-CH_3); 22.3 (-S-CH_2-); 46.9 (dmso); 55.4 (-OCH_3); 112.9 (=CH); 118.3 (-Ar-*o*-C); 129.7 (-Ar-*m*-C/-Ar-C1); 135.7 (-Ar-*p*-C); 159.9 (-Ar-OCH_3); 174.5 (-C-O-); 177.6 (-C=S). MS (ESI): m/z = 579, 413, 393, 301.Elemental analysis: calculated for $C_{14}H_{19}ClO_3PtS_3$·1/2 acetone C: 31.5%; H: 3.75%; S: 16.27%, found: C: 32.02%; H: 3.75%; S: 16.76%.

Chloro-(1-(4-methoxyphenyl)-3-(ethylthio)-3-thioxo-prop-1-en-1-olate-*O,S*)-(dimethylsulfoxide-*S*)-platinum(II) (Pt6).

Synthesis was performed according to general procedure 1, pathway A. L6 (389 mg, 1.53 mmol) was dissolved in THF, *t*-BuOK (172 mg, 1.53 mmol) was added. K_2PtCl_4 (700 mg, 1.69 mmol) was dissolved in water, dmso (220 µL, 3.07 mmol) was added. Column chromatography mobile phase: DCM 4:pentane 1 - DCM - DCM 2:acetone1- -acetone. Yield: 150 mg (17.5%) as yellow crystals. ^{1}H NMR (400 MHz, $CDCl_3$): δ = 1.42 (t, 3H, -S-CH_2-CH_3); 3.24 (q, 2H, -S-CH_2-); 3.63 (s w/Pt satellites $^{3}J_{Pt-H}$=22.5 Hz, 6H, CH_3 (dmso)); 3.83 (s, 3H, -OCH_3); 6.89 (d, $^{3}J_{H-H}$=9.0 Hz, 2H, -Ar-*o*-H); 7.07 (s, 1H, =CH); 7.95 (d, $^{3}J_{H-H}$=9.0 Hz, 2H, -Ar-*m*-H).

^{13}C{^{1}H} NMR (101 MHz, $CDCl_3$): δ = 13.3 (-S-CH_2-CH_3); 22.3 (-S-CH_2-); 46.8 (dmso); 55.5 (-OCH_3); 111.0 (=CH); 114.1 (-Ar-*o*-C); 129.4 (-Ar-C1); 130.2 (-Ar-*m*-C); 163.0 (-Ar-OCH_3); 174.2 (-C-O-); 177.9 (-C=S). MS (ESI): m/z = 579, 413, 393, 301.Elemental analysis: calculated for $C_{14}H_{19}ClO_3PtS_3$·1/3 pentane C: 32.11%; H: 3.96%; S: 16.41%, found: C: 32.43%; H: 3.73%; S: 16.52%.

View Article Online
DOI: 10.1039/C6DT01388K

Chloro-(1-(3-hydroxyphenyl)-3-(methylthio)-3-thioxo-prop-1-en-1-olate-*O,S*)-(dimethylsulfoxide-*S*)-platinum(II) (Pt7).

Synthesis was performed according to general procedure 1, pathway A and B. L7 (350 mg, 1.53 mmol) was dissolved in THF, *t*-BuOK (172 mg, 1.53 mmol) was added. K_2PtCl_4 (700 mg, 1.70 mmol) was dissolved in water, dmso (220 µL, 3.07 mmol) was added. Column chromatography mobile phase: DCM - acetone 20:DCM 1 - acetone 10:DCM 1 — acetone 2:DCM 1. Yield: 380 mg (46.4%) as orange crystals.

^{1}H NMR (600 MHz, acetone-d_6): δ = 2.63 (s, 3H, -S-CH_3); 3.61 (s w/Pt satellites $^3J_{Pt\text{-}H}$=22.5 Hz, 6H, CH_3 (dmso)); 7.02 (dd, $^3J_{H\text{-}H}$=8.2 Hz, $^4J_{H\text{-}H}$=0.8 Hz, 1H, -Ar-*p*-H); 7.15 (s, 1H, =CH); 7.24 (t, 1H, -Ar-*m*-H); 7.47 (m, 2H, -Ar-*o*-H); 8.73 (s, 1H, -Ar-OH).^{13}C{^{1}H} NMR (101 MHz, acetone-d_6): δ = 16.7 (-S-CH_3); 45.9 (dmso); 110.8 (=CH); 114.6 (-Ar-*o*-C); 118.6 (-Ar-*o*-C); 119.3 (-Ar-C1); 130.1 (-Ar-*m*-C); 138.6 (-Ar-*p*-C); 157.9 (-Ar-OH); 174.2 (-C-O-); 177.6 (-C=S). MS (ESI): m/z = 516, 471, 413, 359, 301, 215. MS (DEI): m/z = 279, 167, 149, 121, 113, 83, 71, 57, 43. Elemental analysis: calculated for $C_{12}H_{17}ClO_3PtS_3$·1/3 acetone C: 28.22%; H: 3.09%; S:17.38%, found: C: 28.53%; H:2.82%; S: 17.95%.

Chloro-(1-(4-hydroxyphenyl)-3-(methylthio)-3-thioxo-prop-1-en-1-olate-*O,S*)-(dimethylsulfoxide-*S*)-platinum(II) (Pt8).

Synthesis was performed according to general procedure 1, pathway A and B. L8 (248 mg, 1.10 mmol) was dissolved in THF, *t*-BuOK (123 mg, 1.10 mmol) was added. K_2PtCl_4 (500 mg, 1.21 mmol) was dissolved in water, dmso (160 µL, 2.20 mmol) was added. Column chromatography mobile phase:DCM 2:pentane 1 - DCM 1 - acetone 20:DCM 1 - acetone 10:DCM 1 - acetone 2:DCM 1. Yield: 210 mg (35.8%) as yellow crystals. ^{1}H NMR (600 MHz, acetone-d_6): δ = 2.61 (s, 3H, -S-CH_3); 3.60 (s w/Pt satellites $^3J_{Pt\text{-}H}$=22.5 Hz, 6H, CH_3 (dmso)); 6.85 (d, $^3J_{H\text{-}H}$=9.0 Hz, 2H, -Ar-*o*-H); 7.16 (s, 1H, =CH); 7.95 (d, $^3J_{H\text{-}H}$=9.0 Hz, 2H, -Ar-*m*-H).

^{13}C{^{1}H} NMR (101 MHz, acetone-d_6): δ = 16.7 (-S-CH_3); 45.9 (dmso); 109.9 (=CH); 115.7 (-Ar-*o*-C); 128.3 (-Ar-C1); 130.5 (-Ar-*m*-C); 161.7 (-Ar-C-OH); 174.2 (-C-O-); 178.7 (-C=S). MS (ESI): m/z = 530, 471, 413, 359, 301, 194, 121. MS (DEI): m/z = 528, 382, 327, 279, 194, 179, 167, 136, 121, 78. Elemental analysis: calculated for $C_{12}H_{17}ClO_3PtS_3$·1/3 pentane C: 29.42%; H: 3.43%; S:17.24%, found: C: 29.93%; H:3.01%; S: 16.80%.

Chloro-(1-(3-hydroxyphenyl)-3-(ethylthio)-3-thioxo-prop-1-en-1-olate-*O,S*)-(dimethylsulfoxide-*S*)-platinum(II) (Pt9).

Synthesis was performed according to general procedure 1, pathway A and B. L9 (369 mg, 1.53 mmol) was dissolved in THF, *t*-BuOK (172 mg, 1.53 mmol) was added. K_2PtCl_4 (700 mg, 1.70 mmol) was dissolved in water, dmso (220 µL, 3.07 mmol) was added. Column chromatography mobile phase: DCM 2:pentane 1 - DCM 1 - acetone 20:DCM 1 - acetone 10:DCM 1 - Acetone 2:DCM 1. Yield: 130 mg (15.5%) as yellow crystals. ^{1}H NMR (600 MHz, acetone-d_6): δ = 1.37 (t, 3H, -S-CH_2-CH_3); 3.22 (q, 2H, -S-CH_2-); 3.61 (s w/Pt

View Article Online
DOI: 10.1039/C6DT01388K

satellites $^{3}J_{Pt\text{-}H}$=22.5 Hz, 6H, CH_3 (dmso)); 7.03 (d, $^{3}J_{H\text{-}H}$=8.1 Hz, 1H, -Ar-*p*-H); 7.15 (s, 1H, =CH); 7.24 (t, 1H, -Ar-*m*-H); 7.46 (m, 2H, -Ar-*o*-H); 8.74 (s, 1H, Ar-C-OH).$^{13}C\{^{1}H\}$ NMR (101 MHz, acetone-d_6): δ = 12.8 (-S-CH_2-CH_3); 25.9 (-S-CH_2-); 45.9 (dmso); 111.0 (=CH); 114.4 (-Ar-*o*-C); 119.6 (-Ar-C1); 120.2 (-Ar-*o*-C); 129.7 (-Ar-*m*-C); 138.8 (-Ar-*p*-C); 156.9 (-Ar-C-OH); 174.5 (-C-O-); 196.8 (-C=S). MS (ESI): m/z = 510, 434, 359, 301, 289, 197, 78. MS (DEI): m/z = 298, 268, 239, 213, 208, 181, 179, 167, 138, 136, 98, 93, 78, 63, 61, 29. Elemental analysis: calculated for $C_{12}H_{17}ClO_3PtS_3$·1/10 pentane C: 29.2%; H: 3.30%; S: 17.33%, found: C: 29.44%; H: 3.02%; S: 17.38%.

Chloro-(1-(4-hydroxyphenyl)-3-(ethylthio)-3-thioxo-prop-1-en-1-olate-*O,S*)-(dimethylsulfoxide-*S*)-platinum(II) (Pt10).

Synthesis was performed according to general procedure 1, pathway A and B. L10 (369 mg, 1.53 mmol) was dissolved in THF, *t*-BuOK (172 mg, 1.53 mmol) was added. K_2PtCl_4 (700 mg, 1.70 mmol) was dissolved in water, dmso (220 µL, 3.07 mmol) was added. Column chromatography mobile phase: DCM 1 - acetone 20:DCM 1 - acetone 10:DCM 1 - Acetone 2:DCM 1. Yield: 130 mg (15.5%) as yellow crystals.

^{1}H NMR (600 MHz, acetone-d_6): δ = 1.35 (t, 3H, -S-CH_2-CH_3); 3.20 (q, 2H, -S-CH_2-); 3.60 (s w/Pt satellites $^{3}J_{Pt\text{-}H}$=22.5 Hz, 6H, CH_3 (dmso)); 6.85 (m, 2H, -Ar-*o*-H); 7.16 (s, 1H, =CH); 7.82 (d, $^{3}J_{H\text{-}H}$=9.0 Hz, 2H, -Ar-*m*-H); 9.24 (s, 1H, Ar-C-OH). $^{13}C\{^{1}H\}$ NMR (101 MHz, acetone-d_6): δ = 12.9 (-S-CH_2-CH_3); 28.1 (-S-CH_2-); 45.9 (dmso); 110.3 (=CH); 115.0 (-Ar-*o*-C); 128.4 (-Ar-C1); 129.7 (-Ar-*m*-C); 161.7 (-Ar-C-OH); 174.5 (-C-O-); 177.6 (-C=S). MS (ESI): m/z =, 471, 413, 359, 301, 194, 139. MS (DEI): m/z = 530, 359, 267, 167, 149, 136, 121, 93, 78, 63, 45, 29. Elemental analysis: calculated for $C_{12}H_{17}ClO_3PtS_3$·2,5 acetone C: 35.52%; H: 4.65%; S: 13.88%, found: C: 35.71%; H: 4.08%; S: 14.68%.

Chloro-(1-phenyl-3-(methylthio)-3-thioxo-prop-1-en-1-olate-*O,S*)-(dimethylsulfoxide-*S*)-platinum(II) (Pt11).

Synthesis was performed according to general procedure 1, pathway A. L11 (322 mg, 1.53 mmol) was dissolved in THF, *t*-BuOK (172 mg, 1.53 mmol) was added. K_2PtCl_4 (700 mg, 1.69 mmol) was dissolved in water, dmso (220 µL, 3.07 mmol) was added. Column chromatography mobile phase: DCM 4:hexane 1 - DCM - DCM 1:acetone 1 — acetone. Yield: 330 mg (41.5%) as yellow crystals. ^{1}H NMR (600 MHz, acetone-d_6): δ = 2.70 (s, 3H, -S-CH_3); 3.68 (s w/Pt satellites $^{3}J_{Pt\text{-}H}$=22.5 Hz, 6H, CH_3 (dmso)); 7.28 (s, 1H, =CH); 7.49 (m, 2H, -Ar-*o*-H); 7.62 (m, 1H, -Ar-*p*-H); 8.08 (m, 2H, -Ar-*m*-H). $^{13}C\{^{1}H\}$ NMR (101 MHz, acetone-d_6): δ = 17.8 (-S-CH_3); 46.9 (dmso); 111.6 (=CH); 128.2 (-Ar-*m*-C/-Ar-*p*-C); 128.8 (-Ar-*o*-C); 133.0 (-Ar-C1); 175.1 (-C-O-); 177.6 (-C=S). MS (DEI): m/z = 518, 517, 504, 341, 209, 207, 105, 78, 63, 45. Elemental analysis: calculated for $C_{12}H_{15}ClO_2PtS_3$·1/3 acetone/1/3 $CHCl_3$ C: 27.75%; H: 3.02%; S: 16.67%, found: C: 27.88%; H:2.72%; S: 17.02%.

View Article Online
DOI: 10.1039/C6DT01388K

Chloro-(1-phenyl-3-(ethylthio)-3-thioxo-prop-1-en-1-olate-*O,S*)-(dimethylsulfoxide-*S*)-platinum(II) (Pt12).

Synthesis was performed according to general procedure 1, pathway A. L12 (343 mg, 1.53 mmol) was dissolved in THF, *t*-BuOK (172 mg, 1.53 mmol) was added. K_2PtCl_4 (700 mg, 1.69 mmol) was dissolved in water, dmso (220 µL, 3.07 mmol) was added. Column chromatography mobile phase: DCM 4:hexane 1 - DCM - DCM 1:acetone 1 - acetone. Yield: 470 mg (57.5%) as red crystals. ^{1}H NMR (600 MHz, acetone-d_6): δ = 1.43 (t, 3H, -CH_2-CH_3); 3.29 (q, 2H, -S-CH_2-); 3.67 (s w/Pt satellites $^3J_{Pt\text{-}H}$=22.5 Hz, 6H, CH_3 (dmso)); 7.27 (s, 1H, =CH); 7.49 (m, 2H, -Ar-*o*-H); 7.62 (m, 1H, -Ar-*p*-H); 8.07 (m, 2H, -Ar-*m*-H). ^{13}C{^{1}H} NMR (101 MHz, acetone-d_6): δ = 13.7 (-S-CH_2-CH_3); 29.2 (-S-CH_2-); 46.8 (dmso); 111.8 (=CH); 128.1 (-Ar-*o*-C); 128.7 (-Ar-*m*-C/-Ar-*p*-C); 138.2 (-Ar-C1); 175.3 (-C-O-); 181.5 (-C=S). MS (DEI): m/z = 518, 517, 504, 341, 209, 207, 105, 78, 63, 45. Elemental analysis: calculated for $C_{12}H_{15}ClO_3PtS_3$·2/3 acetone/1/3 $CHCl_3$ C: 30.17%; H: 3.52%; S: 15.76%, found: C: 30.38%; H: 2.93%; S: 15.68%.

Crystal structure determination

The intensity data for the compounds were collected on a Nonius KappaCCD diffractometer using graphite-monochromated Mo-K_α radiation. Data were corrected for Lorentz and polarization effects; absorption was taken into account on a semi-empirical basis using multiple-scans.[52-54]

The structures were solved by direct methods (SHELXS) and refined by full-matrix least squares techniques against Fo^2 (SHELXL-97).[55] All hydrogen atoms of compound **L1, Pt1** and molecule B of **L7**, the hydrogen atoms bounded to the hydroxy-groups of molecule A of **L7** and **Pt10** were located by difference Fourier synthesis and refined isotropically. All other hydrogen atoms were included at calculated positions with fixed thermal parameters. The crystal of **Pt7** was a non-merohedral twin. The twin law was determined by PLATON to (1.0 0.0 0.129) (0.0 -1.0 0.0) (0.0 0.0 1.0).[56] The contribution of the main component was refined to 0.776(1). Crystallographic data as well as structure solution and refinement details are summarized in Table S1. XP (SIEMENS Analytical X-ray Instruments, Inc.) was used for structure representations.

Supporting Information available: Crystallographic data (excluding structure factors) has been deposited with the Cambridge Crystallographic Data Centre as supplementary publication CCDC-1446182 for **L1**, CCDC-1446183 for **L7**, CCDC-1446184 for **Pt1**, CCDC-1446185 for **Pt2**, CCDC-1446186 for **Pt3**, CCDC-1446187 for **Pt5**, CCDC-1446188 for **Pt6**, CCDC-1446189 for **Pt7**, CCDC-1446190 for **Pt9**, and CCDC-1446191 for Pt**10**. Copies of the data can be obtained free of charge on application to CCDC, 12 Union Road, Cambridge CB2 1EZ, UK [E- mail: deposit@ccdc.cam.ac.uk].

View Article Online
DOI: 10.1039/C6DT01388K

Stability determinations

NMR-spectra were measured via NMR-spectroscopy on Bruker Avance 600 MHz. Substances were solved in dmso-d_6 and measured directly at 37 °C. NMR tubes were incubated at 37 °C and after 24 hours measured again under same conditions.

UV–vis spectra of the compounds at different dmso concentrations and under the conditions used to obtain crystals of HEWL-Pt compounds adducts were registered using a Jasco spectrophotomer at room temperature in cuvette with optical length of 0.1 cm. Spectra of the compounds in 10 mM PBS pH 7.4 and 0.9% NaCl were registered using Cary-win 50 spectrophotomer in cuvette with optical length of 1 cm.

DNA-binding behavior

DNA-binding behavior were measured via NMR-spectroscopy on Bruker Avance 600 MHz by 37 °C. Model base 9-methylguanine was applied from Sigma Aldrich, both compounds (model base as well as platinum(II)-complex) were solved separately in dmso-d_6, quickly mixed and quickly transferred in a NMR tube. Measurements starts directly after the transfer of the single molecules for 24 hours and 30 minutes (NS = 64 (3 minutes and 38 seconds), pause: 390 seconds, 145 experiments). We used 6 mg from complex as well as for the model base, which results in a high molecular excess of the 9-methylguanine, to imitate excesses in the biological system and because of intensity of the signals.

Biological Assays

Ovarian cancer cell lines were cultured under standard conditions (5 % CO2, 37 °C, 90 % humidity) in RPMI medium supplemented with 10 % FCS, 100 U/ml penicillin and 100 µg/ml streptomycin (Life Technologies, Germany). Cisplatin (Sigma, Germany) was freshly dissolved at 1 mg/ml in 0.9 % NaCl solution and diluted appropriately. New Platinum(II) complexes and ligands were dissolved in dmso. Platinum-resistant A2780 and SKOV3 cells were established by repeated rounds of 3 day incubations with increasing amounts of Cisplatin starting with 0.1 µM. The concentration was doubled after 3 incubations interrupted by recovery phases with normal medium. Cells that survived the third round of 12.8 µM Cisplatin were defined as resistant cultures. Determinations of IC50 values were carried out using the CellTiter96 non-radioactive proliferation assay (MTT assay, Promega). After seeding 5000 cells per well in a 96-well plate cells were allowed to attach for 24h and were incubated for 48h with different concentrations of the substances ranging from 0 to 1000 µM for Platinum and 0 to 1000 µM for ligand tests (0, 1, 10, 50, 100, 500, 1000 µm), for Cisplatin from 0 to 100 µM (0.1, 1, 5, 10, 50, 100 µM). Each measurement was done in triplicate and repeated 3-times. The proportion of live cells was quantified by the MTT assay and after background subtraction relative values compared to the mean of medium controls were calculated. Non-linear regression analyses applying the Hill-slope were run in GraphPad 5.0 software.

View Article Online
DOI: 10.1039/C6DT01388K

For the determination of DNA damage induced by the treatment with different substances histone γH2AX foci were visualized by immunocytochemical staining. Cells were seeded on coverslips to reach 60-70% confluence after 24h. After incubation (24h) with different substances at IC_{50} concentrations for the resistant cells, cells were washed 3x with PBS and fixed for 10min in 4% paraformaldehyde. Cells were again washed 3-times and then permeabilised by incubation with 0.25% Triton-X in PBS for 5min. Primary antibody against γH2AX (clone JBW301, Millipore, diluted 1:2000) was incubated for 1h at RT and coverslips were washed 3-times afterwards. Alexa488-labelled secondary anti-mouse antibody (life technologies) was used in a 1:1000 dilution in PBS and applied for 1h at RT. Cells were washed 3-times, counterstained with DAPI, washed again and embedded in mounting medium (Vectorshield, Vector Systems). Slides were stored at 4°C in darkness until microscopic evaluation was done using a Zeiss LSM 710 laser scanning microscope.

Fluorescence

Intrinsic fluorescence spectra of HEWL (0.1 mg x mL^{-1}) in the presence of increasing concentrations of the Pt compounds, at fixed dmso concentration (1.4%), were measured at 25 °C with a Horiba Fluoromax 4, using 5 nm/5 nm slit widths. The excitation wavelength was 280 nm, and the emission wavelength was read at 295–450 nm. The temperature of the sample was maintained by a Peltier-thermostat.

Crystallization of protein-Pt compound adducts

Crystals of hen egg white lysozyme (HEWL)-Pt compound adducts appeared in solutions consisting of 1.1 M NaCl, 0.1 M sodium acetate pH 4.4. Single crystals suitable for X-ray experiments were grown by the hanging drop vapor-diffusion method using a 1:1 ratio of reservoir solution and protein adducts solution with a protein concentration of ~15 mg ml^{-1}.

Data collection, structure determination and refinement

Crystals were flask-cooled in nitrogen in the absence of cryoprotectant, as done in other works (see for example [57]) and then screened for diffraction quality. X-ray data were collected at ~100 K on at the CNR Institute of Biostructure and Bioimages. Data were indexed, integrated and scaled with HKL2000.[52] Details of data processing are reported in Table S3.

The structures were solved using the coordinated from PDB code 4J1A, without water and ligands and the molecular-replacement method as implemented in Phaser.[47, 58] All the models were refined independently using Refmac of the CCP4 suite (see Table 1).[59, 60] Model building and electron density map fitting were performed using WinCoot.[61] Structural figures were prepared using PyMOL (http://www.pymol.org/) Structures were deposited in the Protein Data Bank.

View Article Online
DOI: 10.1039/C6DT01388K

Acknowledgements

The authors would like to thank Ralf Trautwein for fruitful discussions. A.M. would like to thank G. Sorrentino and M. Amendola at CNR Institute of Biostructures and Bioimages for technical assistance.

Notes and references

1. B. Rosenberg, L. Van Camp and T. Krigas, *Nature (London, U. K.)*, 1965, **205**, 698-699.
2. B. Rosenberg, *Interdiscip. Sci. Rev.*, 1978, **3**, 134.
3. M. Galanski and B. K. Keppler, *Anti-Cancer Agents Med. Chem.*, 2007, **7**, 55-73.
4. R. A. Alderden, M. D. Hall and T. W. Hambley, *J Chem Educ*, 2006, **83**, 728-734.
5. J. Reedijk, *Inorg. Chim. Acta*, 1992, **198-200**, 873-881.
6. E. R. Jamieson and S. J. Lippard, *Chem. Rev. (Washington, D. C.)*, 1999, **99**, 2467-2498.
7. A. Gadducci, S. Cosio, S. Muraca and A. R. Genazzani, *Eur J Gynaecol Oncol*, 2002, **23**, 390-396.
8. M. A. Fuertes, J. Castilla, C. Alonso and J. M. Perez, *Curr. Med. Chem.*, 2003, **10**, 257-266.
9. J. Reedijk, *PNAS*, 2003, **100**, 3611-3616.
10. D. Wang and S. J. Lippard, *Nat. Rev. Drug Discovery*, 2005, **4**, 307-320.
11. S. Ishida, J. Lee, D. J. Thiele and I. Herskowitz, *Proc. Natl. Acad. Sci. U. S. A.*, 2002, **99**, 14298-14302.
12. X. Lin, T. Okuda, A. Holzer and S. B. Howell, *Mol. Pharmacol.*, 2002, **62**, 1154-1159.
13. N. D. Eljack, H.-Y. M. Ma, J. Drucker, C. Shen, T. W. Hambley, E. J. New, T. Friedrich and R. J. Clarke, *Metallomics*, 2014, **6**, 2126-2133.
14. S. E. Miller and D. A. House, *Inorg. Chim. Acta*, 1989, **166**, 189-197.
15. D. Steinhilber, M. Schubert-Zsilavecz and H. J. Roth, Deutscher Apotheker Verlag, 2010.
16. G. Gasser, I. Ott and N. Metzler-Nolte, *J. Med. Chem.*, 2011, **54**, 3-25.
17. D. D. Von Hoff, R. Schilsky, C. M. Reichert, R. L. Reddick, M. Rozencweig, R. C. Young and F. M. Muggia, *Cancer Treat. Rep.*, 1979, **63**, 1527-1531.
18. M. Dabholkar, F. Bostick-Bruton, C. Weber, V. A. Bohr, C. Egwuagu and E. Reed, *J Natl Cancer Inst*, 1992, **84**, 1512-1517.
19. D. Fink, S. Nebel, S. Aebi, H. Zheng, B. Cenni, A. Nehme, R. D. Christen and S. B. Howell, *Cancer Res.*, 1996, **56**, 4881-4886.
20. A. I. Ivanov, J. Christodoulou, J. A. Parkinson, K. J. Barnham, A. Tucker, J. Woodrow and P. J. Sadler, *J. Biol. Chem.*, 1998, **273**, 14721-14730.
21. D. Hanahan and R. A. Weinberg, *Cell (Cambridge, Mass.)*, 2000, **100**, 57-70.
22. E. Reed, *Clin. Cancer Res.*, 2005, **11**, 6100-6102.
23. J. Helleman, S. I. L. van, W. N. M. Dinjens, K. P. F. van, K. Ritstier, P. C. Ewing, d. B. M. E. L. van, G. Stoter and E. M. J. J. Berns, *BMC Cancer*, 2006, **6**, 201.
24. L. Kelland, *Nat. Rev. Cancer*, 2007, **7**, 573-584.
25. M. Yu, J. Han, P. Cui, M. Dai, H. Li, J. Zhang and R. Xiu, *Cancer Sci.*, 2008, **99**, 391-397.
26. D. Hanahan and R. A. Weinberg, *Cell (Cambridge, MA, U. S.)*, 2011, **144**, 646-674.
27. G. Ciarimboli, *Anticancer Res.*, 2014, **34**, 547-550.
28. C. G. Hartinger and P. J. Dyson, *Chem. Soc. Rev.*, 2009, **38**, 391-401.
29. G. Suess-Fink, *Dalton Trans.*, 2010, **39**, 1673-1688.
30. N. Haefner, D. Steinbach, L. Jansen, H. Diebolder, M. Duerst and I. B. Runnebaum, *Int. J. Cancer*, 2015, Ahead of Print.
31. S. S. G. E. van Boom and J. Reedijk, *J. Chem. Soc., Chem. Commun.*, 1993, 1397-1398.
32. J. Reedijk, *Chem. Rev. (Washington, D. C.)*, 1999, **99**, 2499-2510.
33. C. Muegge, R. Liu, H. Goerls, C. Gabbiani, E. Michelucci, N. Ruediger, J. H. Clement, L. Messori and W. Weigand, *Dalton Trans.*, 2014, **43**, 3072-3086.

View Article Online
DOI: 10.1039/C6DT01388K

34. F. C. V. Larsson and S. O. Lawesson, *Tetrahedron*, 1972, **28**, 5341-5357.
35. W. Weigand, R. Saumweber and P. Schulz, *Z. Naturforsch., B: Chem. Sci.*, 1993, **48**, 1080-1088.
36. R. Saumweber, C. Robl and W. Weigand, *Inorg. Chim. Acta*, 1998, **269**, 83-90.
37. K. Schubert, R. Saumweber, H. Goerls and W. Weigand, *Z. Anorg. Allg. Chem.*, 2003, **629**, 2091-2096.
38. K. Schubert, T. Alpermann, T. Niksch, H. Goerls and W. Weigand, *Z. Anorg. Allg. Chem.*, 2006, **632**, 1033-1042.
39. K. Schubert, H. Goerls and W. Weigand, *Z. Naturforsch., B: Chem. Sci.*, 2007, **62**, 475-482.
40. C. Muegge, T. Marzo, L. Massai, J. Hildebrandt, G. Ferraro, P. Rivera-Fuentes, N. Metzler-Nolte, A. Merlino, L. Messori and W. Weigand, *Inorg. Chem.*, 2015, **54**, 8560-8570.
41. H. Motschi, P. S. Pregosin and H. Ruegger, *J. Organomet. Chem.*, 1980, **193**, 397-405.
42. S. F. Kaplan, V. Y. Kukushkin and A. J. L. Pombeiro, *J. Chem. Soc., Dalton Trans.*, 2001, 3279-3284.
43. D. J. Aitken, A. Albinati, A. Gautier, H.-P. Husson, G. Morgant, D. Nguyen-Huy, J. Kozelka, P. Lemoine, S. Ongeri, S. Rizzato and B. Viossat, *Eur. J. Inorg. Chem.*, 2007, 3327-3334.
44. M. Patra, T. Joshi, V. Pierroz, K. Ingram, M. Kaiser, S. Ferrari, B. Spingler, J. Keiser and G. Gasser, *Chem. - Eur. J.*, 2013, **19**, 14768-14772.
45. E. P. Rogakou, C. Boon, C. Redon and W. M. Bonner, *J. Cell Biol.*, 1999, **146**, 905-915.
46. L. Messori, F. Scaletti, L. Massai, M. A. Cinellu, C. Gabbiani, A. Vergara and A. Merlino, *Chem. Commun. (Cambridge, U. K.)*, 2013, **49**, 10100-10102.
47. A. Vergara, I. Russo Krauss, D. Montesarchio, L. Paduano and A. Merlino, *Inorg. Chem.*, 2013, **52**, 10714-10716.
48. A. Casini, G. Mastrobuoni, C. Temperini, C. Gabbiani, S. Francese, G. Moneti, C. T. Supuran, A. Scozzafava and L. Messori, *Chem. Commun. (Cambridge, U. K.)*, 2007, 156-158.
49. L. Messori, T. Marzo, E. Michelucci, I. Russo Krauss, C. Navarro-Ranninger, A. G. Quiroga and A. Merlino, *Inorg. Chem.*, 2014, **53**, 7806-7808.
50. S. W. M. Tanley, K. Diederichs, L. M. J. Kroon-Batenburg, C. Levy, A. M. M. Schreurs and J. R. Helliwell, *Acta Crystallogr., Sect. F: Struct. Biol. Commun.*, 2014, **70**, 1135-1142.
51. D. Marasco, L. Messori, T. Marzo and A. Merlino, *Dalton Trans.*, 2015, **44**, 10392-10398.
52. Z. Otwinowski and W. Minor, *Methods Enzymol.*, 1997, **276**, 307-326.
53. N. Nonius B.V., 1998.
54. W. Madison, U.S.A, 2002.
55. G. M. Sheldrick, *Acta Crystallogr., Sect. A: Found. Crystallogr.*, 2008, **64**, 112-122.
56. A. L. Spek, *Acta Crystallogr., Sect. D: Biol. Crystallogr.*, 2009, **65**, 148-155.
57. I. Russo Krauss, L. Messori, M. A. Cinellu, D. Marasco, R. Sirignano and A. Merlino, *Dalton Trans.*, 2014, **43**, 17483-17488.
58. A. J. McCoy, R. W. Grosse-Kunstleve, P. D. Adams, M. D. Winn, L. C. Storoni and R. J. Read, *J. Appl. Crystallogr.*, 2007, **40**, 658-674.
59. G. N. Murshudov, P. Skubak, A. A. Lebedev, N. S. Pannu, R. A. Steiner, R. A. Nicholls, M. D. Winn, F. Long and A. A. Vagin, *Acta Crystallogr., Sect. D: Biol. Crystallogr.*, 2011, **67**, 355-367.
60. M. D. Winn, C. C. Ballard, K. D. Cowtan, E. J. Dodson, P. Emsley, P. R. Evans, R. M. Keegan, E. B. Krissinel, A. G. W. Leslie, A. McCoy, S. J. McNicholas, G. N. Murshudov, N. S. Pannu, E. A. Potterton, H. R. Powell, R. J. Read, A. Vagin and K. S. Wilson, *Acta Crystallogr., Sect. D: Biol. Crystallogr.*, 2011, **67**, 235-242.
61. P. Emsley, B. Lohkamp, W. G. Scott and K. Cowtan, *Acta Crystallogr., Sect. D: Biol. Crystallogr.*, 2010, **66**, 486-501.

View Article Online
DOI: 10.1039/C6DT01388K